

# Higgs Searches in WW and ZZ

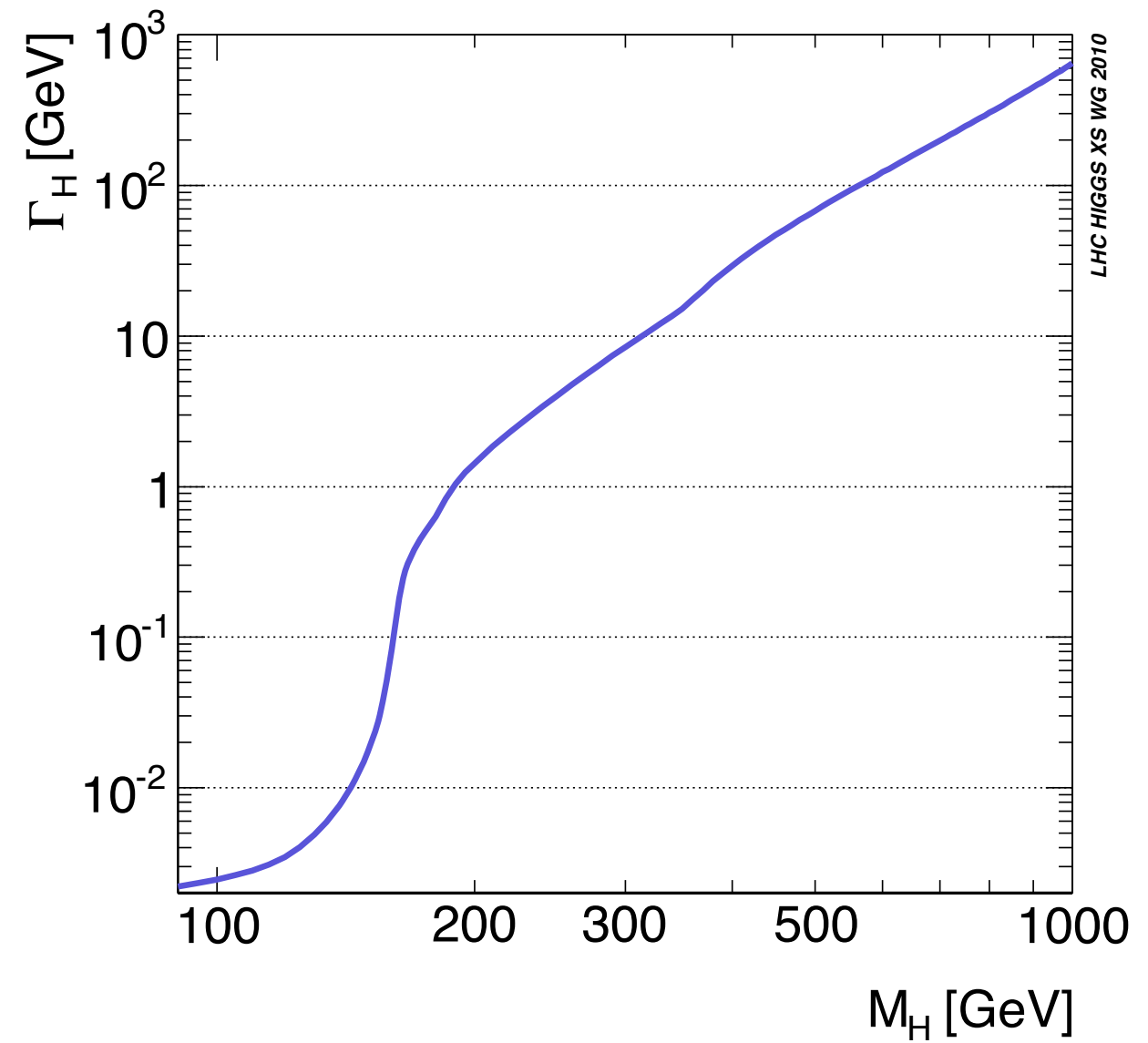
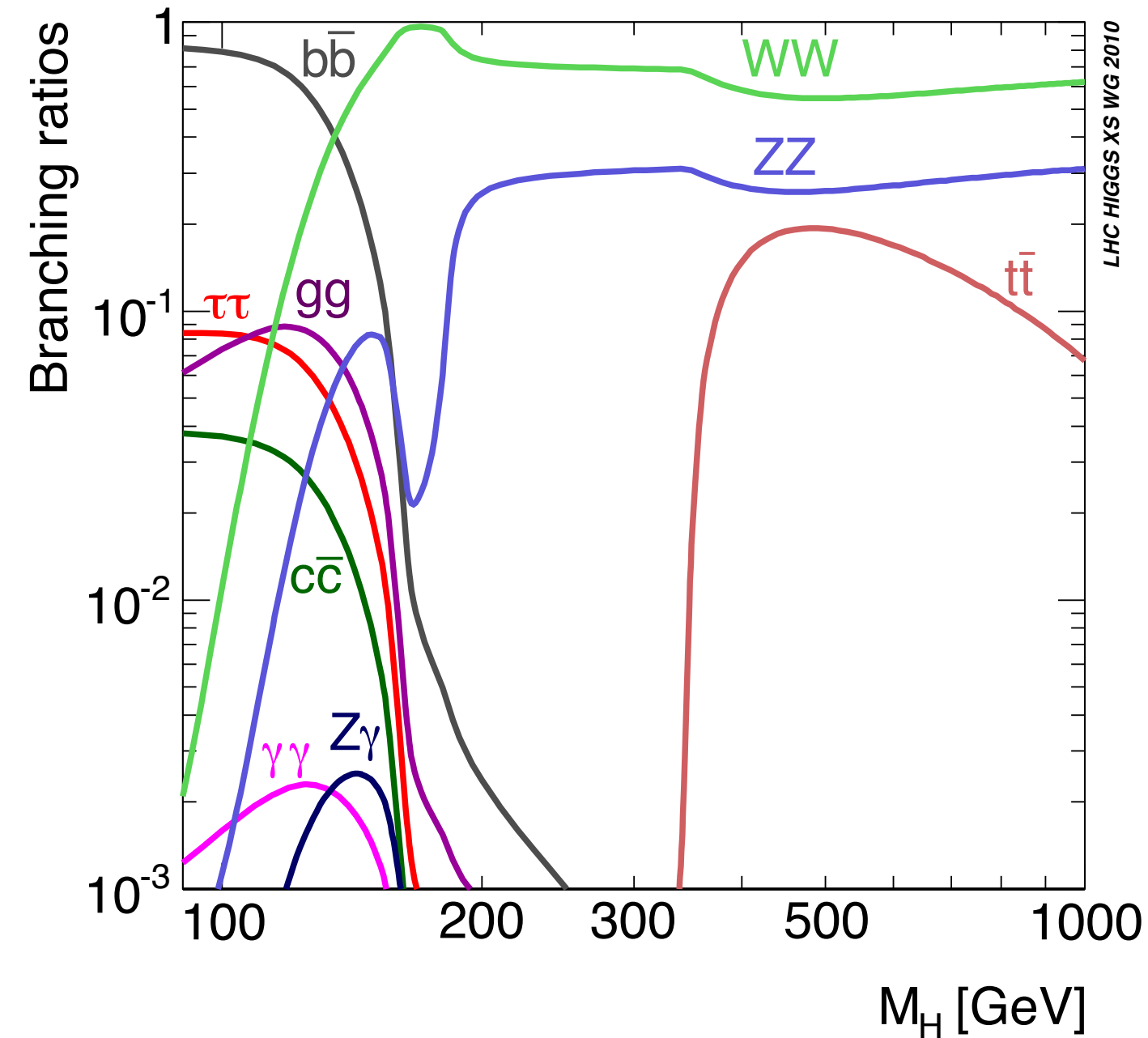
Antonio Boveia, University of Chicago

Chicago LHC Workshop

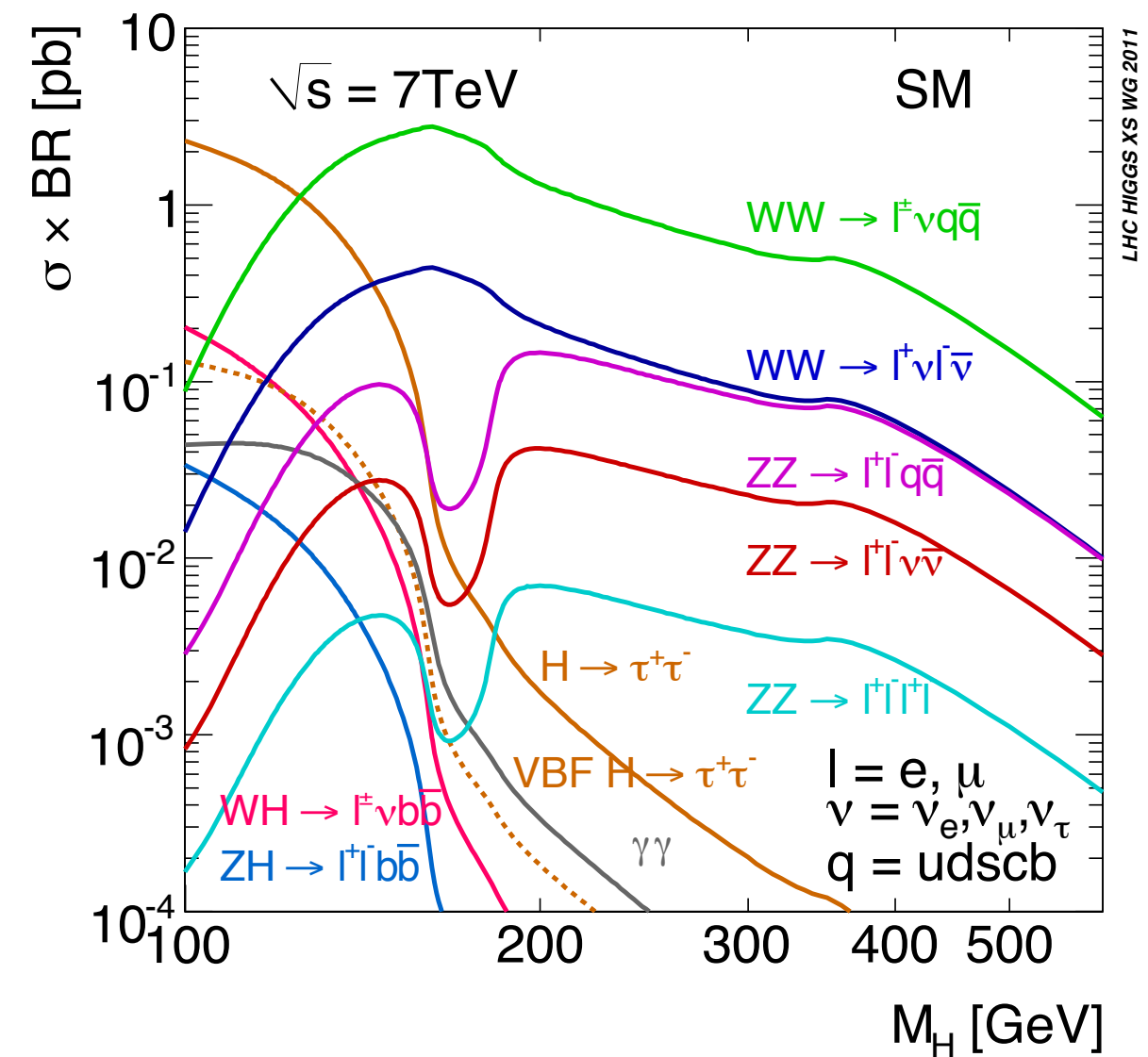
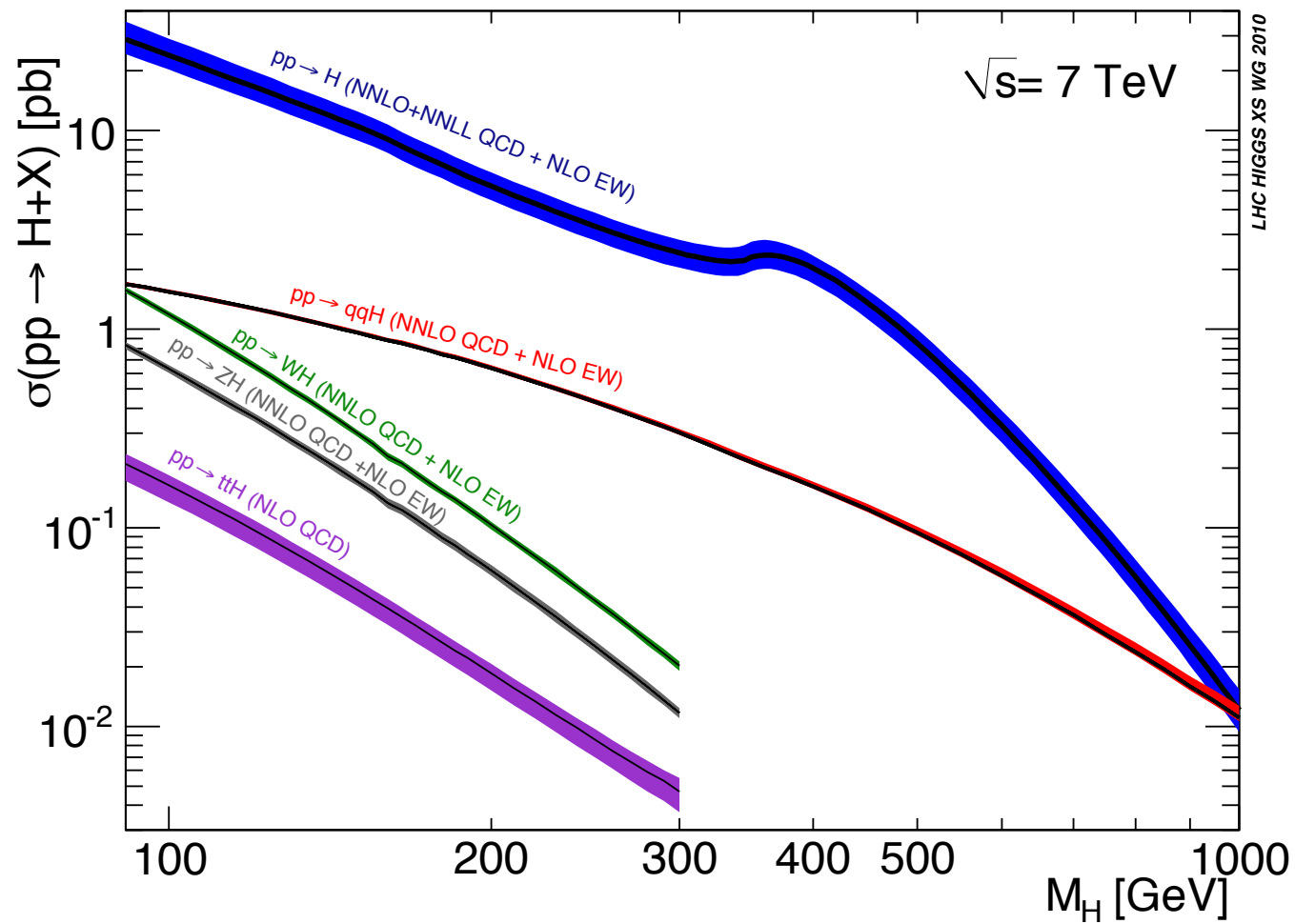
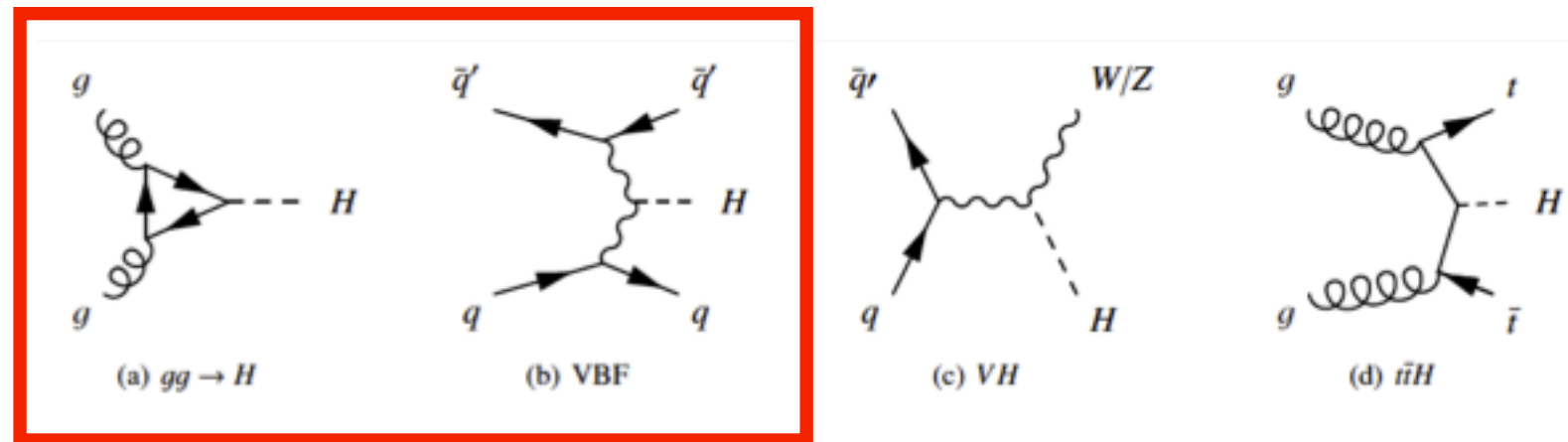
4 May 2012

**Reminder: why search for the Higgs in WW or ZZ specifically?**

**WW and ZZ are by far the dominant decays at high mass...**



... and contribute many signal events even at very low Higgs masses.



• Sweet spot at  $M_H \sim 2 M_W$

## **Reminder: why search for the Higgs in WW or ZZ specifically?**

- *VV mode advantages:*
  - *Large fraction of all effective production at almost all masses*

## Reminder: why search for the Higgs in WW or ZZ specifically?

- *VV mode advantages:*
  - Large fraction of all effective production at almost all masses
  - $ZZ \rightarrow llll, llqq$  fully reconstructible, can (eventually) provide angular information (spin);  $llll$  has very good mass resolution
- *Disadvantages:* WW has poor mass resolution and large backgrounds. ZZ has low branching fraction.
- Without something like the Higgs,  $W_L W_L$  scattering amplitude violates unitarity at large  $s$ 
  - $V_L V_L$  couplings to the Higgs are vital

arXiv:1202.1415

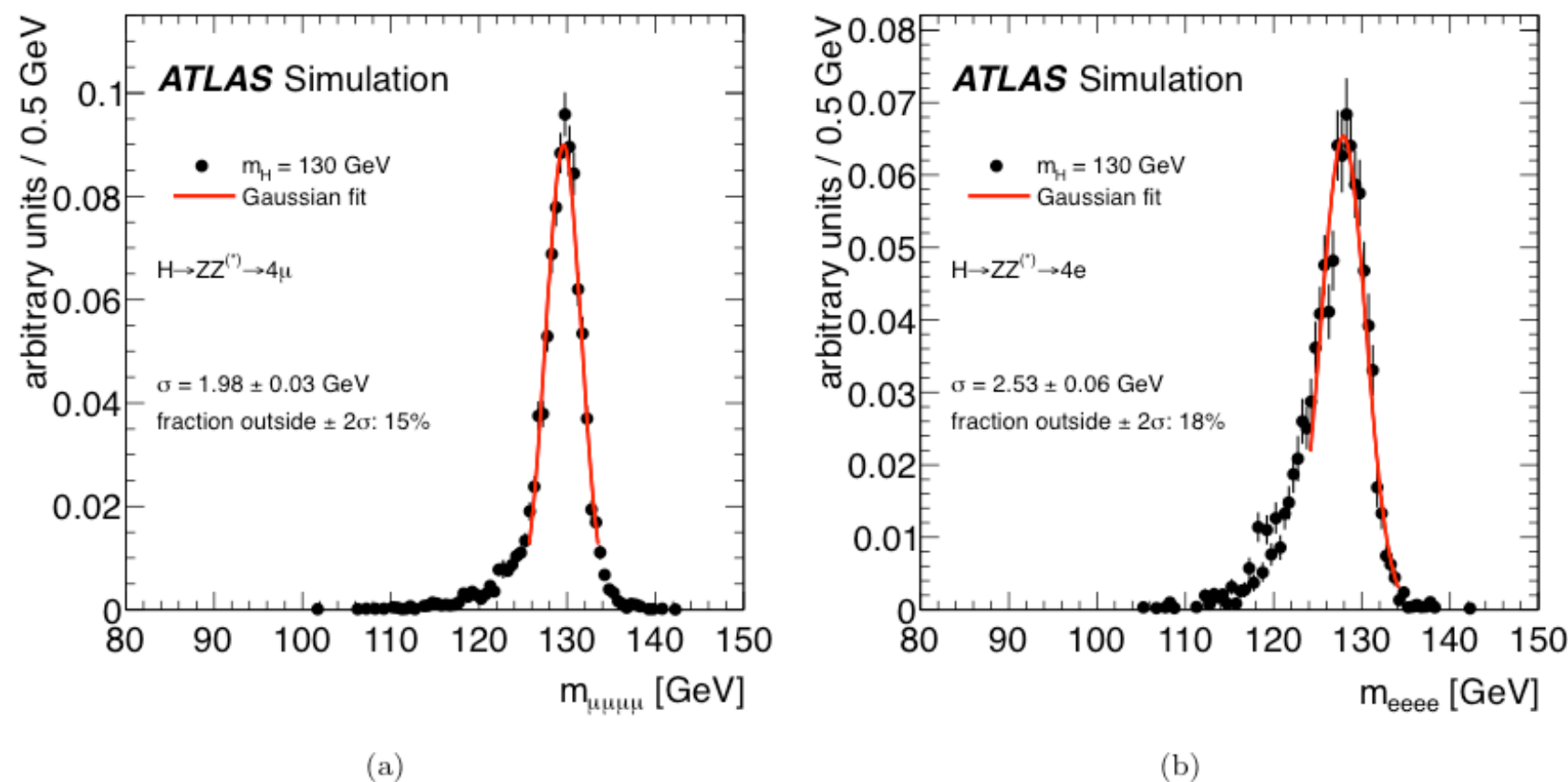


Figure 1: Invariant mass distributions for simulated (a)  $H \rightarrow ZZ^{(*)} \rightarrow 4\mu$  and (b)  $H \rightarrow ZZ^{(*)} \rightarrow 4e$  events for  $m_H = 130$  GeV. The fitted range for the Gaussian is chosen to be :  $-2\sigma$  to  $2\sigma$  ( $-1.5\sigma$  to  $2.5\sigma$ ) for the  $4\mu$  ( $4e$ ) channel. The reduced mean value of the reconstructed invariant mass in the  $4e$  channel arises from energy losses due to bremsstrahlung [76]. The fraction of events outside the  $\pm 2\sigma$  region is found to be 15% for  $4\mu$  and 18% for  $4e$ .

## Reminder: why search for the Higgs in WW or ZZ specifically?

- *VV mode advantages:*
  - *Large fraction of all effective production at almost all masses*
  - *ZZ- $\rightarrow$ llll, llqq fully reconstructible, can (eventually) provide angular information (spin); llll has very good mass resolution*
- *Disadvantages: WW has poor mass resolution and large backgrounds. ZZ has low branching fraction.*
- *Without something like the Higgs,  $W_L W_L$  scattering amplitude violates unitarity at large  $s$* 
  - *$V_L V_L$  couplings to the Higgs are vital*

## Narrow scope

- *Focus on WW- $\rightarrow$  ll+MET and ZZ- $\rightarrow$  llll in this talk*  
*Most important of the WW/ZZ channels to  $M_H=115-130$  GeV*
- *WW- $\rightarrow$  llqq, ZZ- $\rightarrow$  ll+MET, ZZ- $\rightarrow$  llqq results also available but will not be discussed here.*

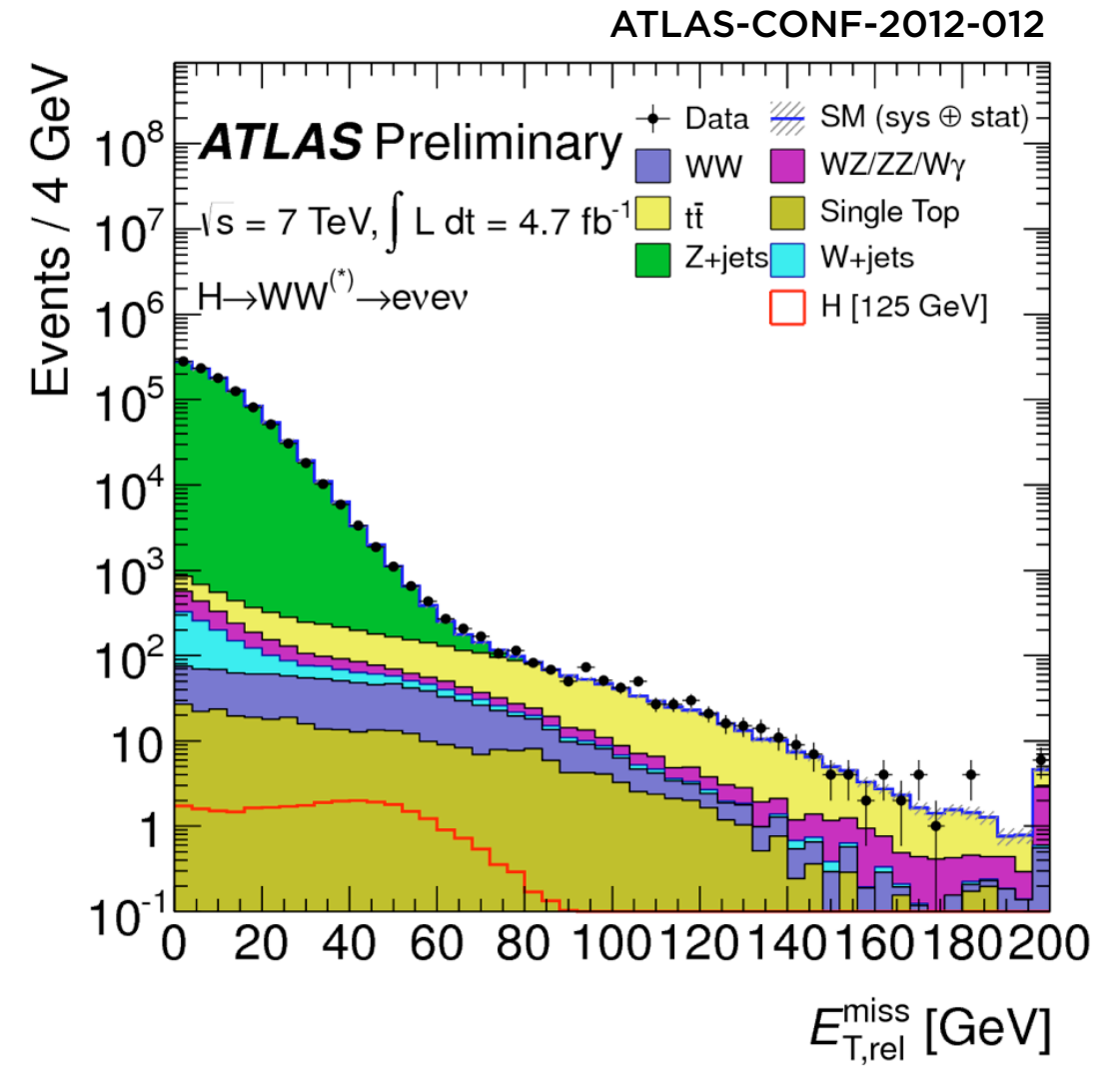
## **WW searches—the ingredients**

- *Select two leptons + some missing  $E_T$*



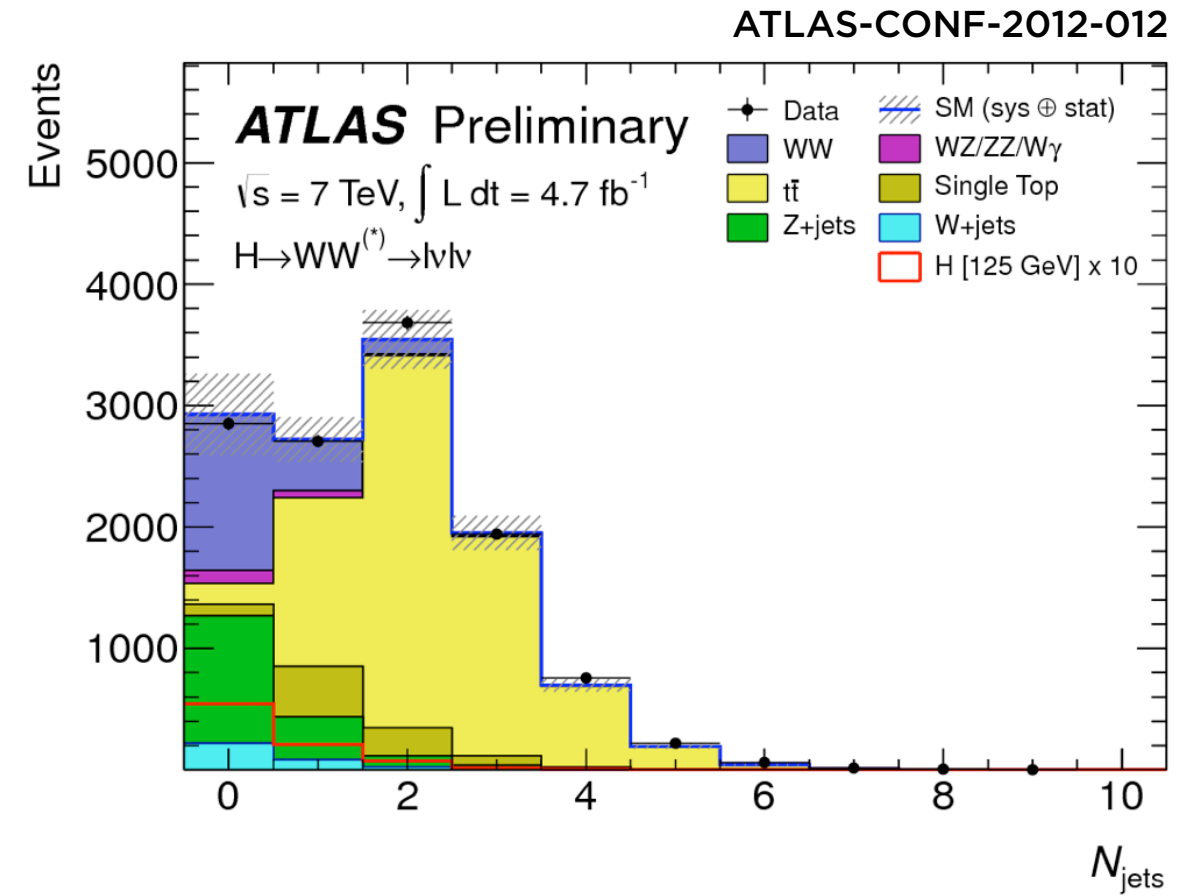
## WW searches—the ingredients

- *Select two leptons + some missing  $E_T$* 
  - $M_H < 160 \text{ GeV} \Rightarrow$  on-shell  $W$  + off-shell  $W^*$  (lower  $p_T$  subleading lepton)
- *Require high missing  $E_T$  and low  $m_{ll}$  to suppress Drell-Yan*



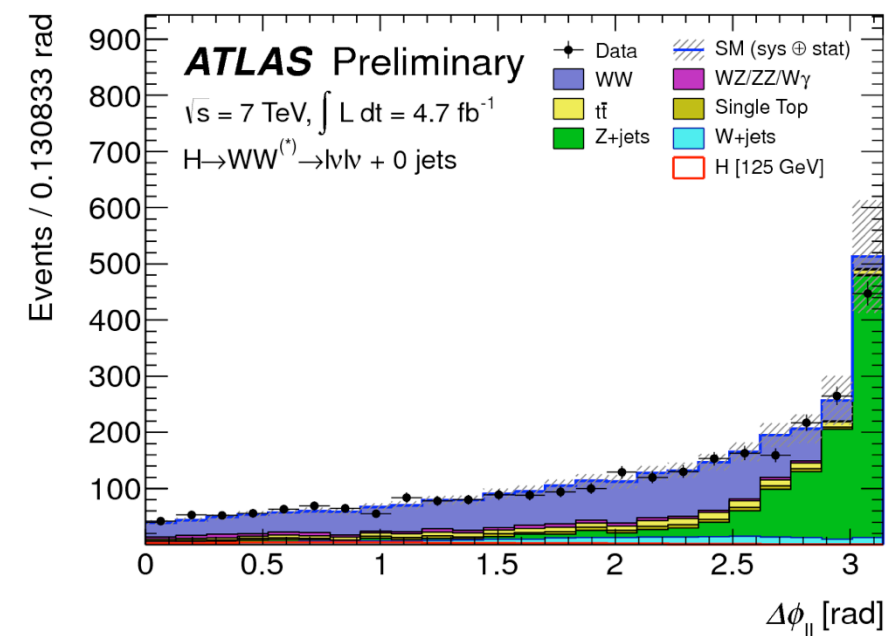
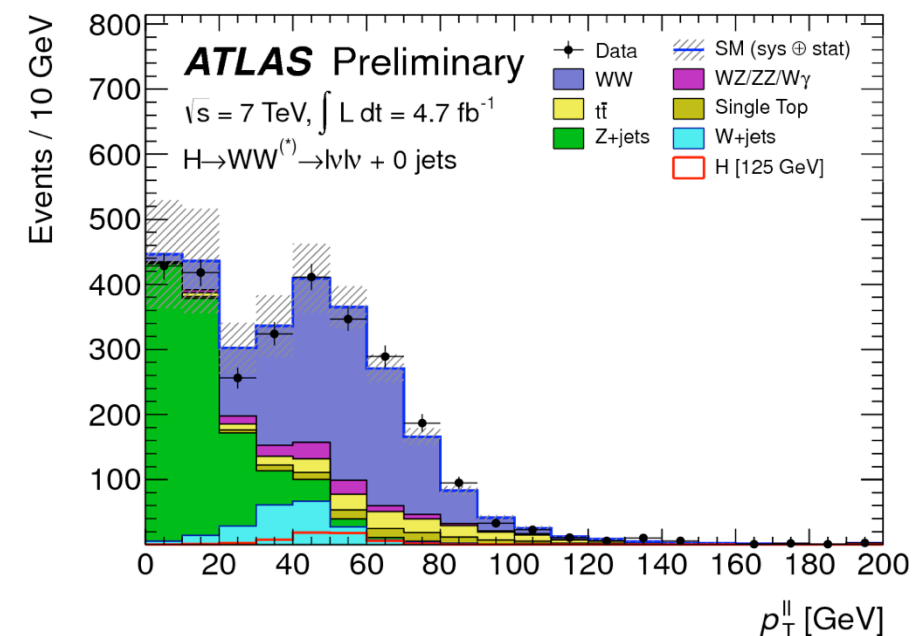
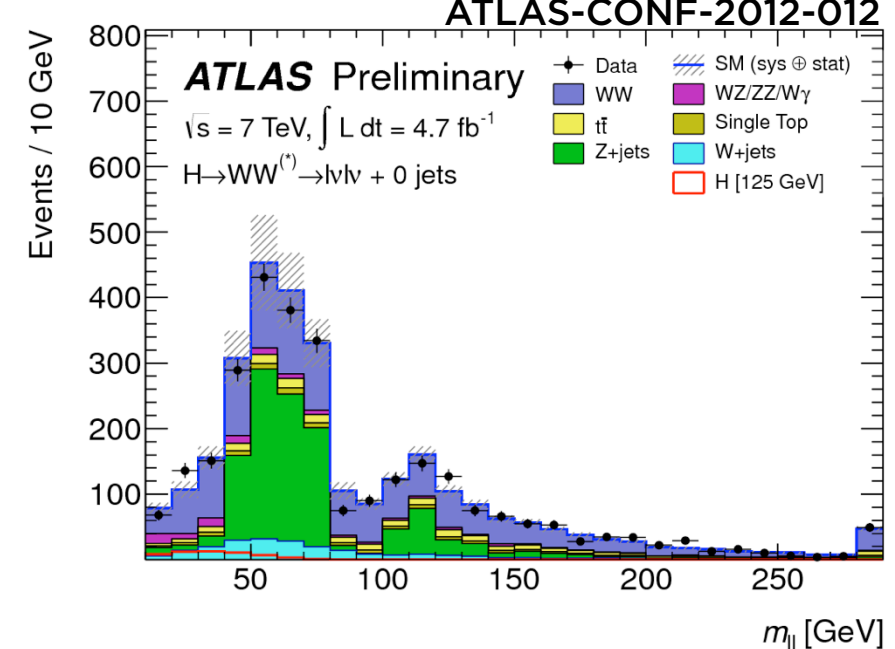
## WW searches—the ingredients

- *Select two leptons + some missing  $E_T$* 
  - $M_H < 160 \text{ GeV} \Rightarrow$  on-shell  $W$  + off-shell  $W^*$  (lower  $p_T$  subleading lepton)
- *Require high missing  $E_T$  and low  $m_{ll}$  to suppress Drell-Yan*
- *Require few jets / no  $b$  tags to suppress top*



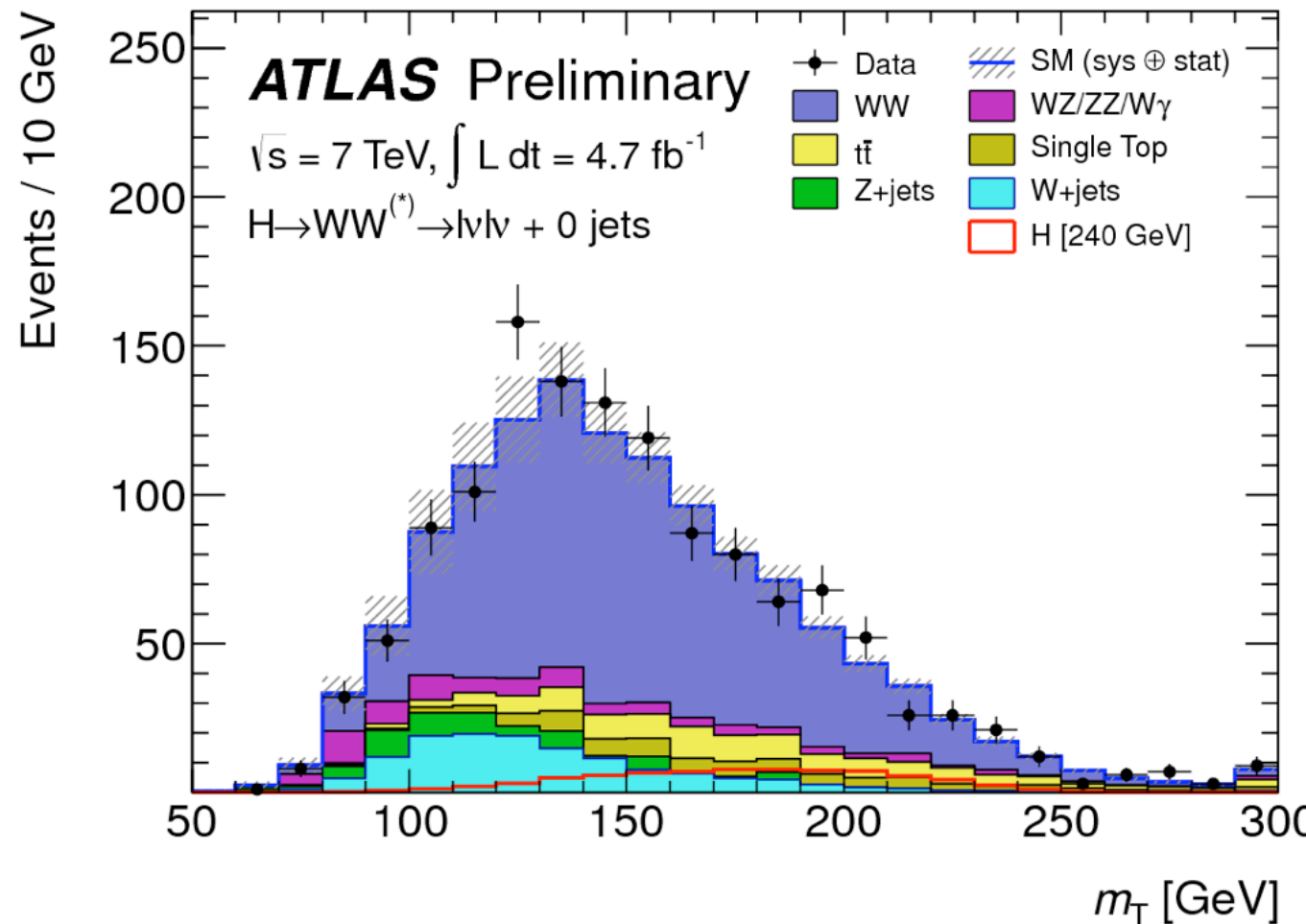
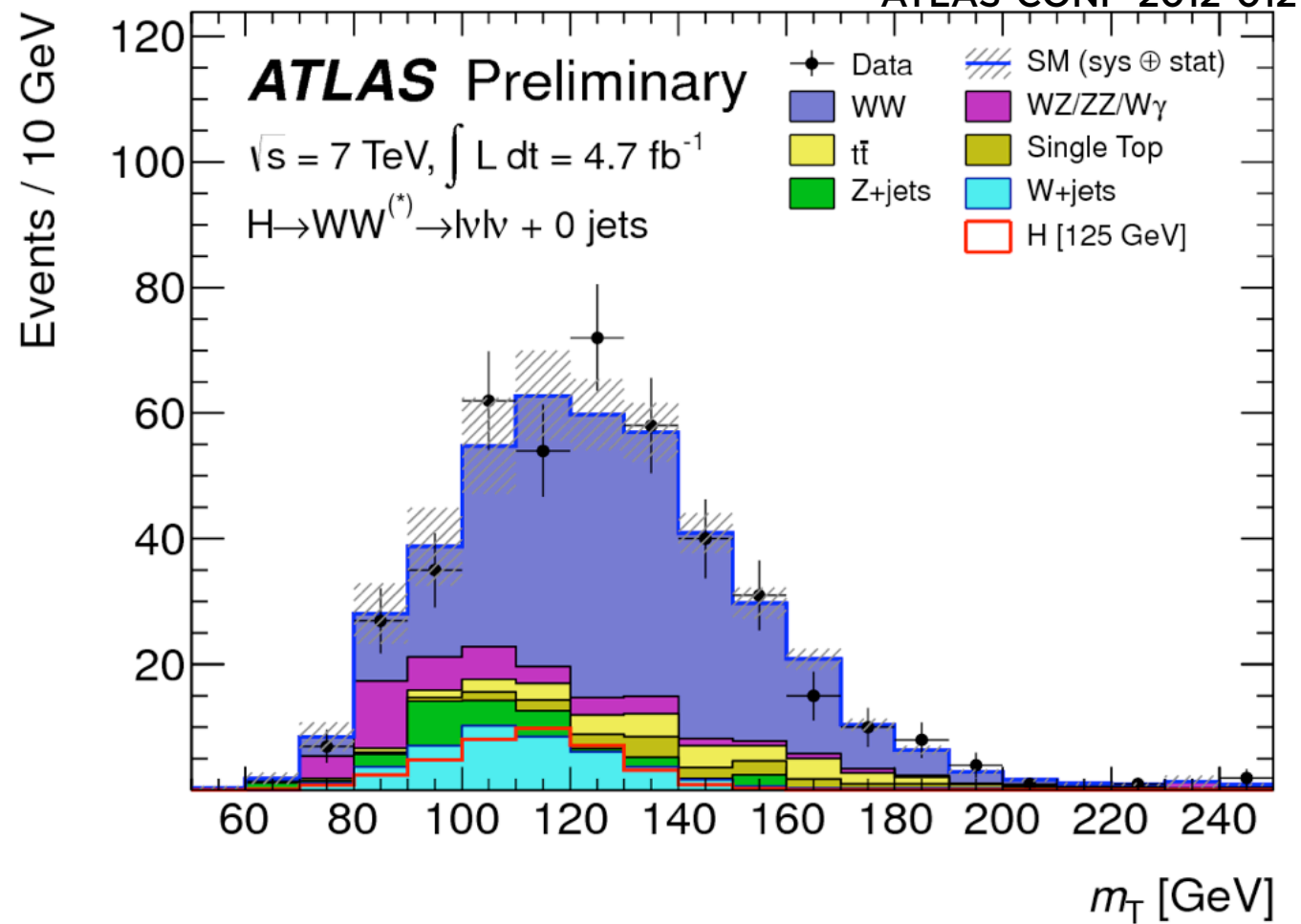
# WW searches—the ingredients

- *Select two leptons + some missing  $E_T$* 
  - $M_H < 160 \text{ GeV} \Rightarrow$  on-shell  $W$  + off-shell  $W^*$  (lower  $p_T$  subleading lepton)
- *Require high missing  $E_T$  and low  $m_{ll}$  to suppress Drell-Yan*
- *Require few jets / no  $b$  tags to suppress top*
- *Require high  $p_T^{ll}$ , narrower window of  $m_{ll}$ , and low  $|\Delta\phi_{ll}|$  to select back-to-back topology, exploit (scalar) angular distribution*



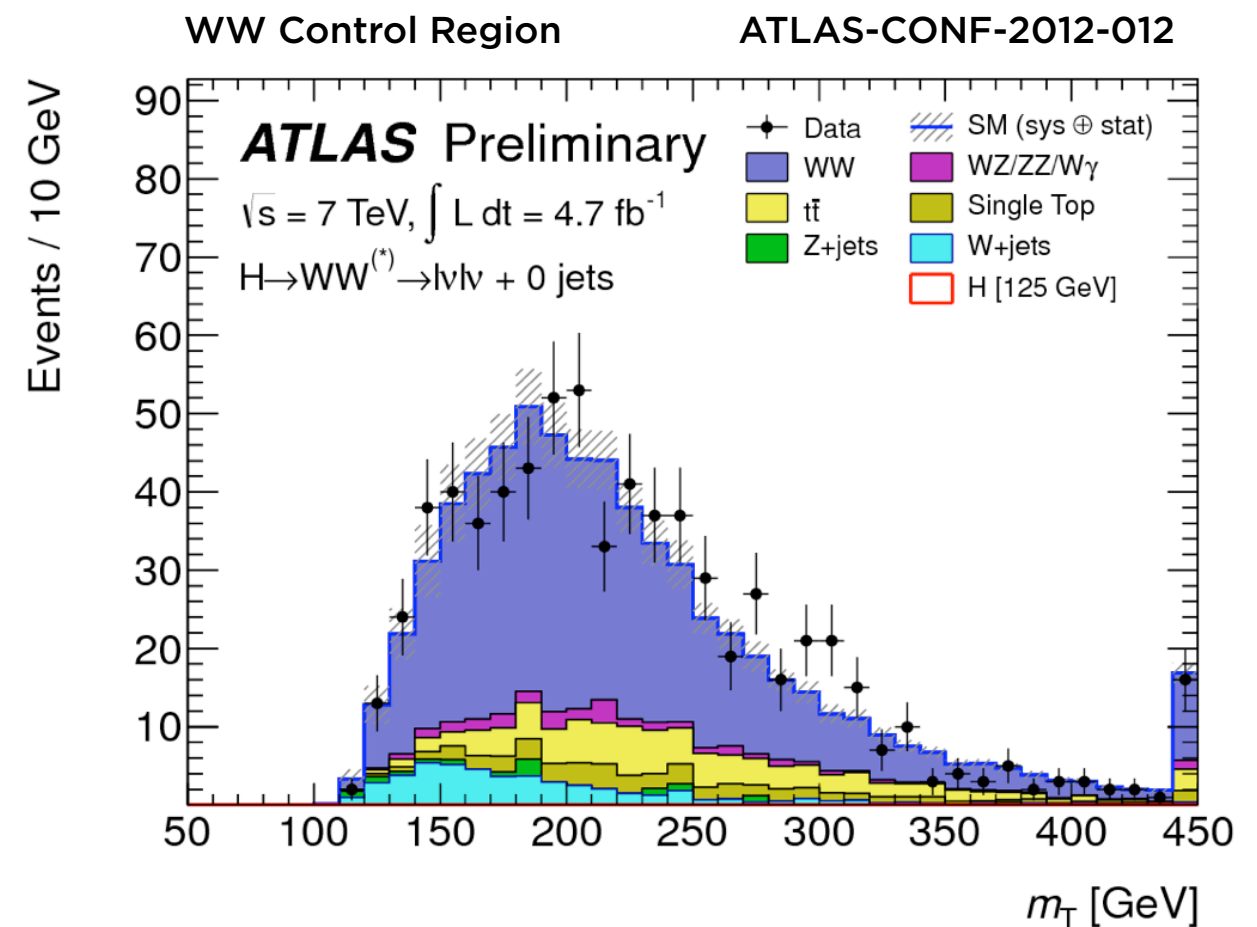
## WW searches—the ingredients

- *Select two leptons + some missing  $E_T$* 
  - $M_H < 160 \text{ GeV} \Rightarrow$  on-shell  $W$  + off-shell  $W^*$  (lower  $p_T$  subleading lepton)
- *Require high missing  $E_T$  and low  $m_{ll}$  to suppress Drell-Yan*
- *Require few jets / no  $b$  tags to suppress top*
- *Require high  $p_T^{ll}$ , narrower window of  $m_{ll}$ , and low  $|\Delta\phi_{ll}|$  to select back-to-back topology, exploit (scalar) angular distribution*
- *Examine transverse mass of two leptons and missing  $E_T$*



# WW searches—the ingredients

- *Select two leptons + some missing  $E_T$* 
  - $M_H < 160 \text{ GeV} \Rightarrow$  on-shell  $W$  + off-shell  $W^*$  (lower  $p_T$  subleading lepton)
- *Require high missing  $E_T$  and low  $m_{ll}$  to suppress Drell-Yan*
- *Require few jets / no  $b$  tags to suppress top*
- *Require high  $p_T^{ll}$ , narrower window of  $m_{ll}$ , and low  $|\Delta\phi_{ll}|$  to select back-to-back topology, exploit (scalar) angular distribution*
- *Examine transverse mass of two leptons and missing  $E_T$*
- *Backgrounds predicted using a mixture of control data and simulation*
  - *Both experiments predict  $W$ +jets with a variation of the “fakeable object” technique*
  - *$WW$  normalization from high  $m_{ll}$  control data*
  - *non- $WW$  ( $WZ, ZZ, W\gamma, W\gamma^*$ )*



# WW mode—early estimated sensitivity

Available on CMS information server

CMS NOTE 2006/047



The Compact Muon Solenoid Experiment

## CMS Note

Mailing address: CMS CERN, CH-1211 GENEVA 23, Switzerland



9 January 2006

## Standard Model Higgs Discovery Potential of CMS in the $H \rightarrow WW \rightarrow \ell\nu\ell\nu$ Channel

G. Davatz, M. Dittmar

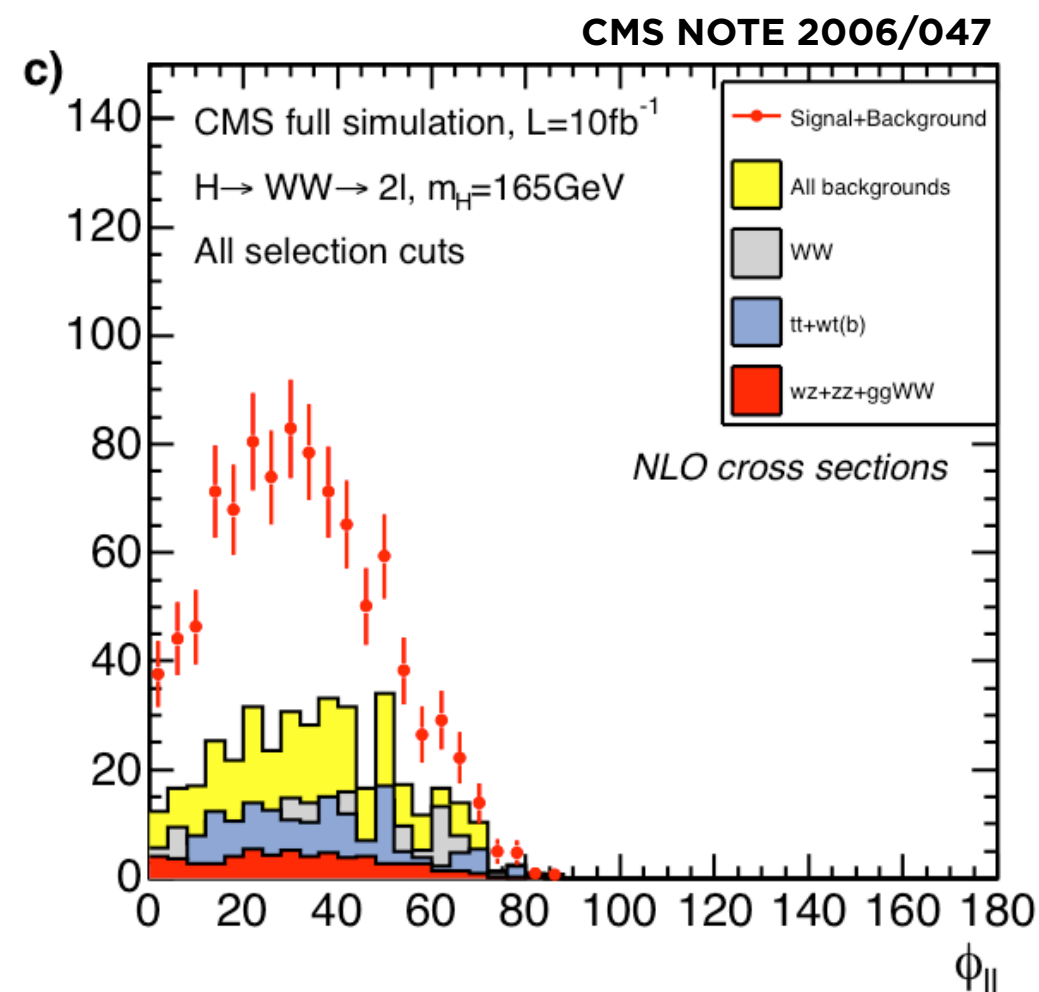
*Institute for Particle Physics, ETH Zürich, Switzerland*

A.-S. Giolo-Nicollérat

*CERN, Geneva, Switzerland*

### Abstract

The discovery potential of the CMS detector for the Standard Model Higgs boson in the  $H \rightarrow WW \rightarrow \ell\nu\ell\nu$  channel is assessed using a full detector simulation. Sources of systematic uncertainties as well as methods to determine backgrounds from data are discussed. If the Standard Model Higgs boson has a mass between 150 GeV and 180 GeV, it should be observed with a significance of more than  $5\sigma$  with a luminosity of about  $10 \text{ fb}^{-1}$ .





## WW mode—early estimated sensitivity

CMS NOTE 2006/047 (14 TeV)

Table 5: The expected number of events for an integrated luminosity of  $1 \text{ fb}^{-1}$  for the signal with Higgs masses between 120 and 160 GeV. The relative efficiency with respect to the previous cut is given in parentheses. The last line shows the total selection efficiency together with the uncertainty from the limited Monte Carlo statistics.

	$H \rightarrow WW$ $m_H = 120 \text{ GeV}$	$H \rightarrow WW$ $m_H = 130 \text{ GeV}$	$H \rightarrow WW$ $m_H = 140 \text{ GeV}$	$H \rightarrow WW$ $m_H = 150 \text{ GeV}$	$H \rightarrow WW$ $m_H = 160 \text{ GeV}$
$\sigma \times \text{BR}(e, \mu, \tau) [\text{fb}]$	560	1060	1570	1970	2330
L1+HLT	247 (44%)	511 (48%)	802 (51%)	1077 (55%)	1353 (58%)
2 lep, $ \eta  < 2$ , $p_t > 20 \text{ GeV}$ $\sigma_{\text{IP}} > 3$ , $ \Delta z_{\text{lep}}  < 0.2 \text{ cm}$	30 (12%)	88 (17%)	171 (21%)	264 (25%)	359 (27%)
$E_t^{\text{miss}} > 50 \text{ GeV}$	12 (39%)	37 (42%)	88 (52%)	150 (57%)	240 (67%)
$\phi_{\ell\ell} < 45$	6.6 (55%)	20 (53%)	44 (50%)	76 (51%)	139 (58%)
$12 \text{ GeV} < m_{\ell\ell} < 40 \text{ GeV}$	5.5 (83%)	15 (76%)	34 (76%)	56 (73%)	107 (77%)
Jet veto	2.3 (41%)	7.4 (50%)	17 (49%)	29 (52%)	56 (52%)
$30 \text{ GeV} < p_t^{\ell \text{ max}} < 55 \text{ GeV}$	1.6 (72%)	5.0 (68%)	13 (77%)	23 (80%)	49 (89%)
$p_t^{\ell \text{ min}} > 25 \text{ GeV}$	0.80 (49%)	3.2 (63%)	8.2 (64%)	17 (75%)	42 (85%)
$\varepsilon_{\text{tot}}$	$(0.14 \pm 0.03)\%$	$(0.30 \pm 0.04)\%$	$(0.52 \pm 0.05)\%$	$(0.86 \pm 0.07)\%$	$(1.80 \pm 0.06)\%$

(CMS also has more recent projections for 7 TeV: [NOTE-2010/008](#))

ATL-PHYS-PUB-2010-009

$M_H (\text{GeV})$	120	130	140	150	160	170	180	190	200
SM WW	26.3	35.4	43.8	50.1	55.2	58.5	60.6	61.7	62.4
top	4.9	6.7	9.1	11.6	14.0	16.3	17.2	17.9	18.2
W+jets	5.6	5.6	5.6	5.6	5.6	5.6	5.6	5.6	5.6
Total background	36.8	47.7	58.5	67.3	74.8	80.4	83.4	85.2	86.2
Signal	4.1	10.4	18.5	26.3	39.5	35.4	26.2	16.8	11.0

Table 6: Estimated number of events for the signal and the major backgrounds at an integrated luminosity of  $1 \text{ fb}^{-1}$  for  $\sqrt{s} = 7 \text{ TeV}$  after the full event selection in  $H \rightarrow WW \rightarrow l\nu l\nu$ .

## WW mode—early estimated sensitivity

CMS NOTE 2006/047 (14 TeV)

Table 8: The signal-to-background ratio for the different Higgs-boson masses together with the integrated luminosity needed for a  $5\sigma$  discovery, with and without the inclusion of background uncertainties. For Higgs masses of 120-140 GeV and 190-200 GeV, the background uncertainties prevent a high significance observation.

$m_H$ [GeV]	S/B	Significance for $5 \text{ fb}^{-1}$		$\mathcal{L}_{\text{disc}}$ [ $\text{fb}^{-1}$ ]		
		no bkg syst	with bkg syst and MC stat	no bkg syst	with bkg syst	with bkg syst and MC stat
120	0.03	0.3	0.2	1100	-	-
130	0.12	1.3	0.7	72	-	-
140	0.30	3.3	1.8	12	-	-
150	0.61	6.6	4.0	3.0	7.1	8.2
160	1.51	14	7.7	0.58	1.0	1.1
165	1.66	15	8.3	0.50	0.81	0.90
170	1.19	11	6.3	0.88	1.5	1.7
180	0.65	6.7	3.7	2.7	5.7	7.3
190	0.33	3.6	2.0	10	-	-
200	0.22	2.2	1.2	27	-	-

ATL-PHYS-PUB-2010-009

$M_H$ (GeV)	120	130	140	150	160	170	180	190	200
Conservative systematics	4.2	1.9	1.2	0.87	0.61	0.71	0.89	1.5	2.0
Optimistic systematics	3.8	1.7	1.0	0.77	0.54	0.62	0.78	1.3	1.8

Table 8: Expected upper limits at 95% CL of the Higgs boson production cross-section normalised to the cross-section predicted by the Standard Model for  $1 \text{ fb}^{-1}$  at  $\sqrt{s} = 7 \text{ TeV}$  and the two systematic uncertainty assumptions used in the  $H \rightarrow WW \rightarrow l\nu l\nu$  analysis.



# WW mode—results

- Divide analyses into bins with very different signal to background:  $ee/\mu\mu/e\mu$ ; 0, 1, or 2 jets

ATLAS-CONF-2012-012

Table 1: The expected numbers of signal and background events after the requirements for the low  $m_H$  selection listed in the first column, as well as the observed numbers of events in data. The signal is for  $m_H = 125$  GeV. The  $W$ +jets background is entirely determined from data, whereas for the other processes the expectations are based on simulation, with  $WW$ ,  $Z/\gamma^*$ +jets,  $t\bar{t}$ , and  $tW/tb/tqb$  normalised using the data control regions as described in the text. Only statistical uncertainties associated with the number of events in the MC samples and the data control regions are shown. The same numbers are shown also in the control regions; here, with the exception of  $W$ +jets, no normalisation scale factors are applied to the expected numbers. The bottom part of the table lists the number of expected and observed events for each lepton channel after the  $\Delta\phi_{\ell\ell}$  cut.

$H + 0\text{-jet}$	Signal	$WW$	$WZ/ZZ/W\gamma$	$t\bar{t}$	$tW/tb/tqb$	$Z/\gamma^* + \text{jets}$	$W + \text{jets}$	Total Bkg.	Obs.
Jet Veto	$54.5 \pm 0.2$	$1285 \pm 79$	$106 \pm 6$	$175 \pm 12$	$95 \pm 7$	$1038 \pm 28$	$217 \pm 4$	$2916 \pm 115$	2851
$m_{\ell\ell} < 50$ GeV	$43.8 \pm 0.2$	$316 \pm 20$	$48 \pm 5$	$30 \pm 2$	$19 \pm 2$	$157 \pm 13$	$69 \pm 2$	$640 \pm 34$	644
$p_T^{\ell\ell}$ cut	$38.8 \pm 0.2$	$285 \pm 18$	$41 \pm 4$	$28 \pm 2$	$18 \pm 2$	$24 \pm 7$	$49 \pm 2$	$444 \pm 27$	441
$\Delta\phi_{\ell\ell} < 1.8$	$37.7 \pm 0.2$	$279 \pm 17$	$39 \pm 4$	$27 \pm 2$	$18 \pm 2$	$23 \pm 7$	$44 \pm 1$	$429 \pm 27$	427
$H + 1\text{-jet}$	Signal	$WW$	$WZ/ZZ/W\gamma$	$t\bar{t}$	$tW/tb/tqb$	$Z/\gamma^* + \text{jets}$	$W + \text{jets}$	Total Bkg.	Obs.
1 jet	$21.1 \pm 0.1$	$390 \pm 55$	$59 \pm 4$	$1433 \pm 80$	$430 \pm 25$	$357 \pm 17$	$82 \pm 3$	$2752 \pm 170$	2707
$b$ -jet veto	$19.5 \pm 0.1$	$360 \pm 51$	$55 \pm 4$	$401 \pm 23$	$134 \pm 8$	$333 \pm 16$	$73 \pm 3$	$1356 \pm 92$	1371
$ \mathbf{p}_T^{\text{tot}}  < 30$ GeV	$13.0 \pm 0.1$	$252 \pm 35$	$33 \pm 3$	$171 \pm 10$	$78 \pm 5$	$105 \pm 8$	$35 \pm 2$	$674 \pm 55$	685
$Z \rightarrow \tau\tau$ veto	$13.0 \pm 0.1$	$246 \pm 34$	$32 \pm 3$	$165 \pm 10$	$75 \pm 5$	$85 \pm 7$	$35 \pm 2$	$638 \pm 53$	645
$m_{\ell\ell} < 50$ GeV	$10.2 \pm 0.1$	$54 \pm 7$	$14 \pm 2$	$32 \pm 2$	$18 \pm 2$	$26 \pm 4$	$12 \pm 1$	$156 \pm 14$	171
$\Delta\phi_{\ell\ell} < 1.8$	$9.4 \pm 0.1$	$49 \pm 7$	$14 \pm 2$	$30 \pm 2$	$17 \pm 2$	$13 \pm 3$	$10 \pm 1$	$134 \pm 13$	145
$H + 2\text{-jet}$	Signal	$WW$	$WZ/ZZ/W\gamma$	$t\bar{t}$	$tW/tb/tqb$	$Z/\gamma^* + \text{jets}$	$W + \text{jets}$	Total Bkg.	Obs.
opp. hemispheres	$3.8 \pm 0.1$	$46 \pm 1$	$6 \pm 1$	$138 \pm 3$	$21 \pm 1$	$34 \pm 4$	$8 \pm 1$	$253 \pm 5$	269
$ \Delta\eta_{jj}  > 3.8$	$1.8 \pm 0.1$	$8.3 \pm 0.4$	$0.9 \pm 0.2$	$19.2 \pm 0.9$	$2.2 \pm 0.4$	$8.0 \pm 2.0$	$1.5 \pm 0.4$	$40.2 \pm 2.3$	40
$m_{jj} > 500$ GeV	$1.3 \pm 0.1$	$3.9 \pm 0.3$	$0.4 \pm 0.1$	$6.9 \pm 0.4$	$0.7 \pm 0.2$	$0.9 \pm 0.4$	$0.7 \pm 0.3$	$13.6 \pm 0.8$	13
$m_{\ell\ell} < 80$ GeV	$0.9 \pm 0.1$	$1.1 \pm 0.2$	$0.1 \pm 0.1$	$1.1 \pm 0.2$	$0.2 \pm 0.1$	$0.3 \pm 0.3$	$0.2 \pm 0.2$	$2.9 \pm 0.5$	2
$\Delta\phi_{\ell\ell} < 1.8$	$0.8 \pm 0.1$	$0.7 \pm 0.1$	$0.1 \pm 0.1$	$0.7 \pm 0.2$	negl.	$0.3 \pm 0.3$	negl.	$1.8 \pm 0.4$	1
Control Regions	Signal	$WW$	$WZ/ZZ/W\gamma$	$t\bar{t}$	$tW/tb/tqb$	$Z/\gamma^* + \text{jets}$	$W + \text{jets}$	Total Bkg.	Obs.
$WW$ 0-jet	$0.1 \pm 0.1$	$465 \pm 3$	$25 \pm 2$	$85 \pm 2$	$41 \pm 2$	$9 \pm 2$	$48 \pm 2$	$673 \pm 5$	698
$WW$ 1-jet	$0.1 \pm 0.1$	$126 \pm 2$	$10 \pm 1$	$83 \pm 2$	$33 \pm 2$	$9 \pm 2$	$11 \pm 1$	$272 \pm 4$	269
Top 1-jet	$1.1 \pm 0.1$	$21 \pm 1$	$1.5 \pm 0.2$	$422 \pm 4$	$165 \pm 3$	$6 \pm 2$	negl.	$615 \pm 6$	675
Lepton Channels		0-jet $ee$	0-jet $\mu\mu$	0-jet $e\mu$	1-jet $ee$	1-jet $\mu\mu$	1-jet $e\mu$		
Total bkg.		$58 \pm 5$	$114 \pm 10$	$257 \pm 13$	$21 \pm 3$	$37 \pm 5$	$76 \pm 6$		
Signal		$3.8 \pm 0.1$	$9.0 \pm 0.1$	$25 \pm 0.2$	$1.1 \pm 0.1$	$2.3 \pm 0.1$	$6.0 \pm 0.1$		
Observed		52	138	237	19	36	90		

# WW mode—results

- Divide analyses into bins with very different signal to background:  $ee/mumu/emu$ ; 0, 1, or 2 jets

CMS-PAS-HIG-11-024

$m_H$	$Z/\gamma^* \rightarrow \ell^+\ell^-$	top	W + jets	WZ + ZZ + $W\gamma$	$pp \rightarrow W^+W^-$	all bkg.	$H \rightarrow W^+W^-$	data
cut-based approach 0-jet category								
120	$8.8 \pm 9.2$	$6.7 \pm 1.0$	$14.7 \pm 4.7$	$6.1 \pm 1.5$	$100.3 \pm 7.2$	$136.7 \pm 12.7$	$15.7 \pm 0.8$	136
130	$13.7 \pm 7.8$	$10.6 \pm 1.6$	$17.6 \pm 5.5$	$7.4 \pm 1.6$	$142.2 \pm 10.0$	$191.5 \pm 14.0$	$45.2 \pm 2.1$	193
160	$3.4 \pm 3.4$	$10.5 \pm 1.4$	$3.0 \pm 1.5$	$2.2 \pm 0.4$	$82.6 \pm 5.4$	$101.7 \pm 6.8$	$122.9 \pm 5.6$	111
200	$2.7 \pm 3.7$	$23.3 \pm 3.1$	$3.4 \pm 1.5$	$3.2 \pm 0.3$	$108.2 \pm 4.5$	$140.8 \pm 6.8$	$48.8 \pm 2.2$	159
250	$0.3 \pm 0.6$	$36.2 \pm 4.8$	$6.7 \pm 2.1$	$5.7 \pm 0.7$	$101.8 \pm 4.5$	$150.8 \pm 6.9$	$23.5 \pm 1.1$	152
300	$0.7 \pm 1.9$	$41.6 \pm 5.4$	$6.5 \pm 2.1$	$7.0 \pm 0.7$	$87.5 \pm 3.9$	$143.3 \pm 7.2$	$20.2 \pm 0.9$	147
400	$0.2 \pm 0.2$	$35.9 \pm 4.7$	$5.5 \pm 1.8$	$9.3 \pm 1.1$	$59.8 \pm 2.7$	$110.8 \pm 5.8$	$17.5 \pm 0.8$	109
cut-based approach 1-jet category								
120	$6.6 \pm 2.3$	$17.2 \pm 1.0$	$5.4 \pm 2.4$	$3.2 \pm 0.6$	$27.0 \pm 4.7$	$59.5 \pm 5.9$	$6.5 \pm 0.3$	72
130	$5.3 \pm 2.5$	$25.6 \pm 1.4$	$6.5 \pm 2.5$	$4.0 \pm 0.6$	$38.5 \pm 6.6$	$79.9 \pm 7.7$	$17.6 \pm 0.8$	105
160	$4.2 \pm 1.4$	$27.9 \pm 1.4$	$3.2 \pm 1.4$	$1.9 \pm 0.3$	$33.7 \pm 5.5$	$70.8 \pm 6.0$	$60.2 \pm 2.6$	86
200	$14.6 \pm 5.3$	$59.4 \pm 2.8$	$5.2 \pm 1.8$	$2.2 \pm 0.1$	$49.3 \pm 2.2$	$130.8 \pm 6.7$	$25.8 \pm 1.1$	111
250	$12.9 \pm 6.8$	$83.8 \pm 3.9$	$5.9 \pm 2.1$	$3.3 \pm 0.2$	$60.3 \pm 2.8$	$166.2 \pm 8.6$	$14.8 \pm 0.6$	158
300	$12.8 \pm 4.8$	$83.6 \pm 3.9$	$6.2 \pm 2.2$	$3.8 \pm 0.4$	$57.5 \pm 2.7$	$163.9 \pm 7.1$	$13.7 \pm 0.6$	168
400	$8.3 \pm 3.2$	$60.6 \pm 2.9$	$6.2 \pm 2.1$	$3.9 \pm 0.5$	$44.6 \pm 2.2$	$123.6 \pm 5.3$	$12.2 \pm 0.5$	128
cut-based approach 2-jet category								
120	$1.9 \pm 1.4$	$5.5 \pm 2.8$	$0.7 \pm 0.6$	$1.8 \pm 1.5$	$1.3 \pm 0.2$	$11.3 \pm 3.6$	$1.1 \pm 0.1$	8
130	$2.7 \pm 1.9$	$6.5 \pm 3.2$	$0.7 \pm 0.6$	$1.8 \pm 1.5$	$1.6 \pm 0.2$	$13.3 \pm 4.0$	$2.7 \pm 0.2$	10
160	$2.7 \pm 1.9$	$8.4 \pm 3.9$	$1.2 \pm 0.8$	$1.8 \pm 1.5$	$1.9 \pm 0.2$	$15.9 \pm 4.6$	$12.2 \pm 0.7$	12
200	$3.2 \pm 2.1$	$9.4 \pm 4.2$	$1.2 \pm 0.8$	$1.8 \pm 1.5$	$2.2 \pm 0.2$	$17.8 \pm 5.0$	$8.4 \pm 0.5$	13
250	$3.3 \pm 2.1$	$12.2 \pm 5.2$	$1.2 \pm 0.8$	$1.9 \pm 1.5$	$3.3 \pm 0.3$	$21.8 \pm 5.9$	$5.6 \pm 0.3$	19
300	$3.3 \pm 2.1$	$14.1 \pm 5.8$	$1.1 \pm 0.8$	$1.9 \pm 1.5$	$3.4 \pm 0.3$	$23.7 \pm 6.4$	$4.2 \pm 0.2$	20
400	$3.3 \pm 2.1$	$14.1 \pm 5.8$	$1.1 \pm 0.8$	$1.9 \pm 1.5$	$3.5 \pm 0.3$	$23.8 \pm 6.4$	$2.5 \pm 0.1$	20

Table 3: Observed number of events, background estimates from the data-driven methods and signal predictions for an integrated luminosity of  $4.6 \text{ fb}^{-1}$  after applying the  $H \rightarrow W^+W^-$  cut-based selection requirements. Only statistical and experimental systematic uncertainties on the processes are reported. The  $Z/\gamma^* \rightarrow \ell^+\ell^-$  process corresponds to the dimuon, dielectron and ditau final states.

# WW mode—results

- Divide analyses into bins with very different signal to background:  $ee/mumu/emu$ ; 0, 1, or 2 jets

CMS-PAS-HIG-11-024

$m_H$	$Z/\gamma^* \rightarrow \ell^+\ell^-$	top	W + jets	WZ + ZZ + $W\gamma$	$pp \rightarrow W^+W^-$	all bkg.	$H \rightarrow W^+W^-$	data
cut-based approach 0-jet category								
120	$8.8 \pm 9.2$	$6.7 \pm 1.0$	$14.7 \pm 4.7$	$6.1 \pm 1.5$	$100.3 \pm 7.2$	$136.7 \pm 12.7$	$15.7 \pm 0.8$	136
130	$13.7 \pm 7.8$	$10.6 \pm 1.6$	$17.6 \pm 5.5$	$7.4 \pm 1.6$	$142.2 \pm 10.0$	$191.5 \pm 14.0$	$45.2 \pm 2.1$	193
160	$3.4 \pm 3.4$	$10.5 \pm 1.4$	$3.0 \pm 1.5$	$2.2 \pm 0.4$	$82.6 \pm 5.4$	$101.7 \pm 6.8$	$122.9 \pm 5.6$	111
200	$2.7 \pm 3.7$	$23.3 \pm 3.1$	$3.4 \pm 1.5$	$3.2 \pm 0.3$	$108.2 \pm 4.5$	$140.8 \pm 6.8$	$48.8 \pm 2.2$	159
250	$0.3 \pm 0.6$	$36.2 \pm 4.8$	$6.7 \pm 2.1$	$5.7 \pm 0.7$	$101.8 \pm 4.5$	$150.8 \pm 6.9$	$23.5 \pm 1.1$	152
300	$0.7 \pm 1.9$	$41.6 \pm 5.4$	$6.5 \pm 2.1$	$7.0 \pm 0.7$	$87.5 \pm 3.9$	$143.3 \pm 7.2$	$20.2 \pm 0.9$	147
400	$0.2 \pm 0.2$	$35.9 \pm 4.7$	$5.5 \pm 1.8$	$9.3 \pm 1.1$	$59.8 \pm 2.7$	$110.8 \pm 5.8$	$17.5 \pm 0.8$	109
cut-based approach 1-jet category								
120	$6.6 \pm 2.3$	$17.2 \pm 1.0$	$5.4 \pm 2.4$	$3.2 \pm 0.6$	$27.0 \pm 4.7$	$59.5 \pm 5.9$	$6.5 \pm 0.3$	72
130	$5.3 \pm 2.5$	$25.6 \pm 1.4$	$6.5 \pm 2.5$	$4.0 \pm 0.6$	$38.5 \pm 6.6$	$79.9 \pm 7.7$	$17.6 \pm 0.8$	105
160	$4.2 \pm 1.4$	$27.9 \pm 1.4$	$3.2 \pm 1.4$	$1.9 \pm 0.3$	$33.7 \pm 5.5$	$70.8 \pm 6.0$	$60.2 \pm 2.6$	86
200	$14.6 \pm 5.3$	$59.4 \pm 2.8$	$5.2 \pm 1.8$	$2.2 \pm 0.1$	$49.3 \pm 2.2$	$130.8 \pm 6.7$	$25.8 \pm 1.1$	111
250	$12.9 \pm 6.8$	$83.8 \pm 3.9$	$5.9 \pm 2.1$	$3.3 \pm 0.2$	$60.3 \pm 2.8$	$166.2 \pm 8.6$	$14.8 \pm 0.6$	158
300	$12.8 \pm 4.8$	$83.6 \pm 3.9$	$6.2 \pm 2.2$	$3.8 \pm 0.4$	$57.5 \pm 2.7$	$163.9 \pm 7.1$	$13.7 \pm 0.6$	168
400	$8.3 \pm 3.2$	$60.6 \pm 2.9$	$6.2 \pm 2.1$	$3.9 \pm 0.5$	$44.6 \pm 2.2$	$123.6 \pm 5.3$	$12.2 \pm 0.5$	128
cut-based approach 2-jet category								
120	$1.9 \pm 1.4$	$5.5 \pm 2.8$	$0.7 \pm 0.6$	$1.8 \pm 1.5$	$1.3 \pm 0.2$	$11.3 \pm 3.6$	$1.1 \pm 0.1$	8
130	$2.7 \pm 1.9$	$6.5 \pm 3.2$	$0.7 \pm 0.6$	$1.8 \pm 1.5$	$1.6 \pm 0.2$	$13.3 \pm 4.0$	$2.7 \pm 0.2$	10
160	$2.7 \pm 1.9$	$8.4 \pm 3.9$	$1.2 \pm 0.8$	$1.8 \pm 1.5$	$1.9 \pm 0.2$	$15.9 \pm 4.6$	$12.2 \pm 0.7$	12
200	$3.2 \pm 2.1$	$9.4 \pm 4.2$	$1.2 \pm 0.8$	$1.8 \pm 1.5$	$2.2 \pm 0.2$	$17.8 \pm 5.0$	$8.4 \pm 0.5$	13
250	$3.3 \pm 2.1$	$12.2 \pm 5.2$	$1.2 \pm 0.8$	$1.9 \pm 1.5$	$3.3 \pm 0.3$	$21.8 \pm 5.9$	$5.6 \pm 0.3$	19
300	$3.3 \pm 2.1$	$14.1 \pm 5.8$	$1.1 \pm 0.8$	$1.9 \pm 1.5$	$3.4 \pm 0.3$	$23.7 \pm 6.4$	$4.2 \pm 0.2$	20
400	$3.3 \pm 2.1$	$14.1 \pm 5.8$	$1.1 \pm 0.8$	$1.9 \pm 1.5$	$3.5 \pm 0.3$	$23.8 \pm 6.4$	$2.5 \pm 0.1$	20

ANALYSIS COMES DOWN TO HOW WE BELIEVE THE NORMALIZATIONS OF SEVERAL TRICKY BACKGROUNDS

(EXPLOITED MOST OF AVAILABLE SHAPE INFORMATION)

ditaus final states.

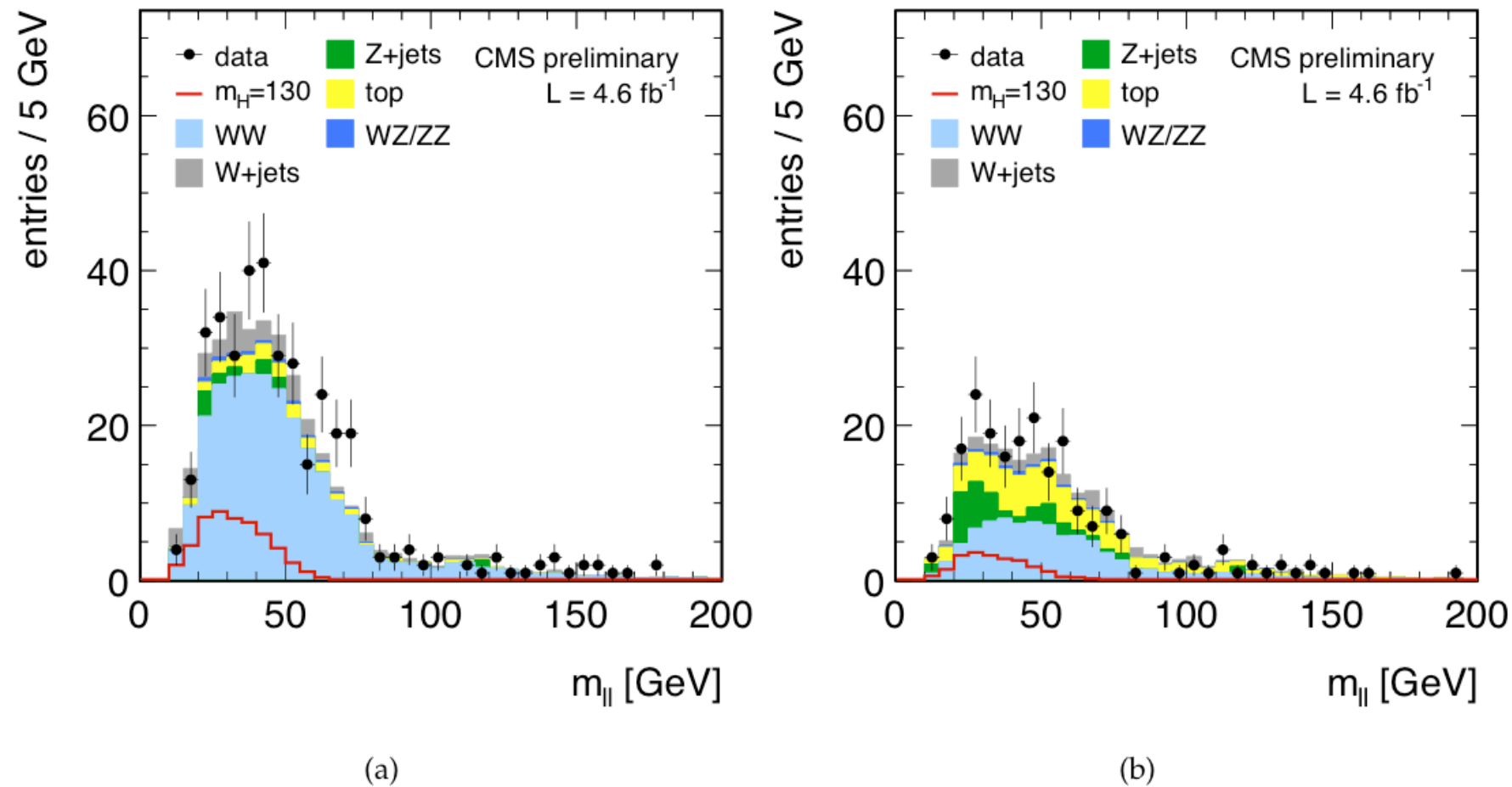


Figure 2: Dilepton mass of the two selected leptons in the 0-jet (a) and 1-jet (b) categories, for  $m_H = 130$  GeV/ $c^2$  SM Higgs hypothesis and for the main backgrounds. The cut-based  $H \rightarrow W^+W^-$  selection except for the cut on the dilepton mass itself is applied. The area marked as  $W^+W^-$  corresponds to non-resonant  $W^+W^-$  production.



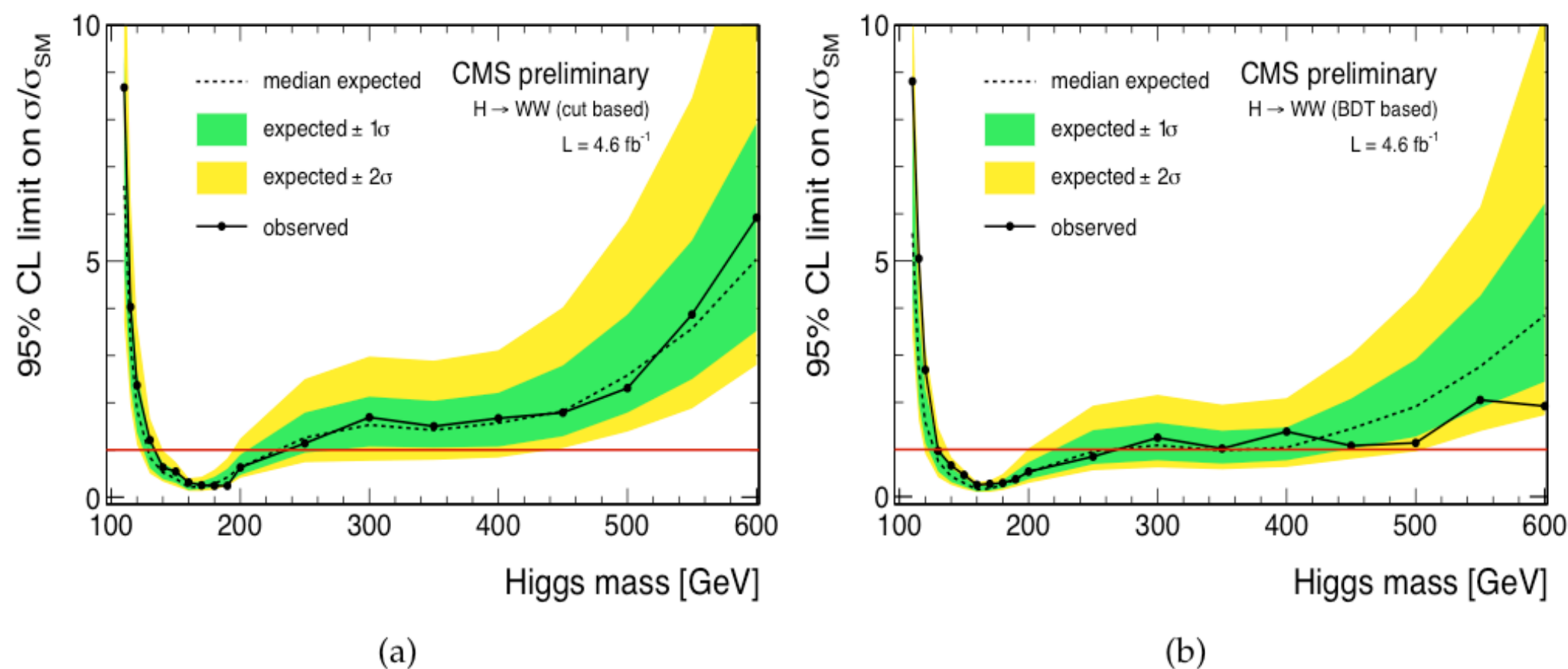


Figure 4: 95% expected and observed C.L. upper limits on the cross section times branching ratio,  $\sigma_{\text{H}} \times \text{BR}(\text{H} \rightarrow \text{W}^+ \text{W}^- \rightarrow 2\ell 2\nu)$ , relative to the SM value using cut-based (a) and multivariate BDT (b) event selections. Results are obtained using the CLs approach.

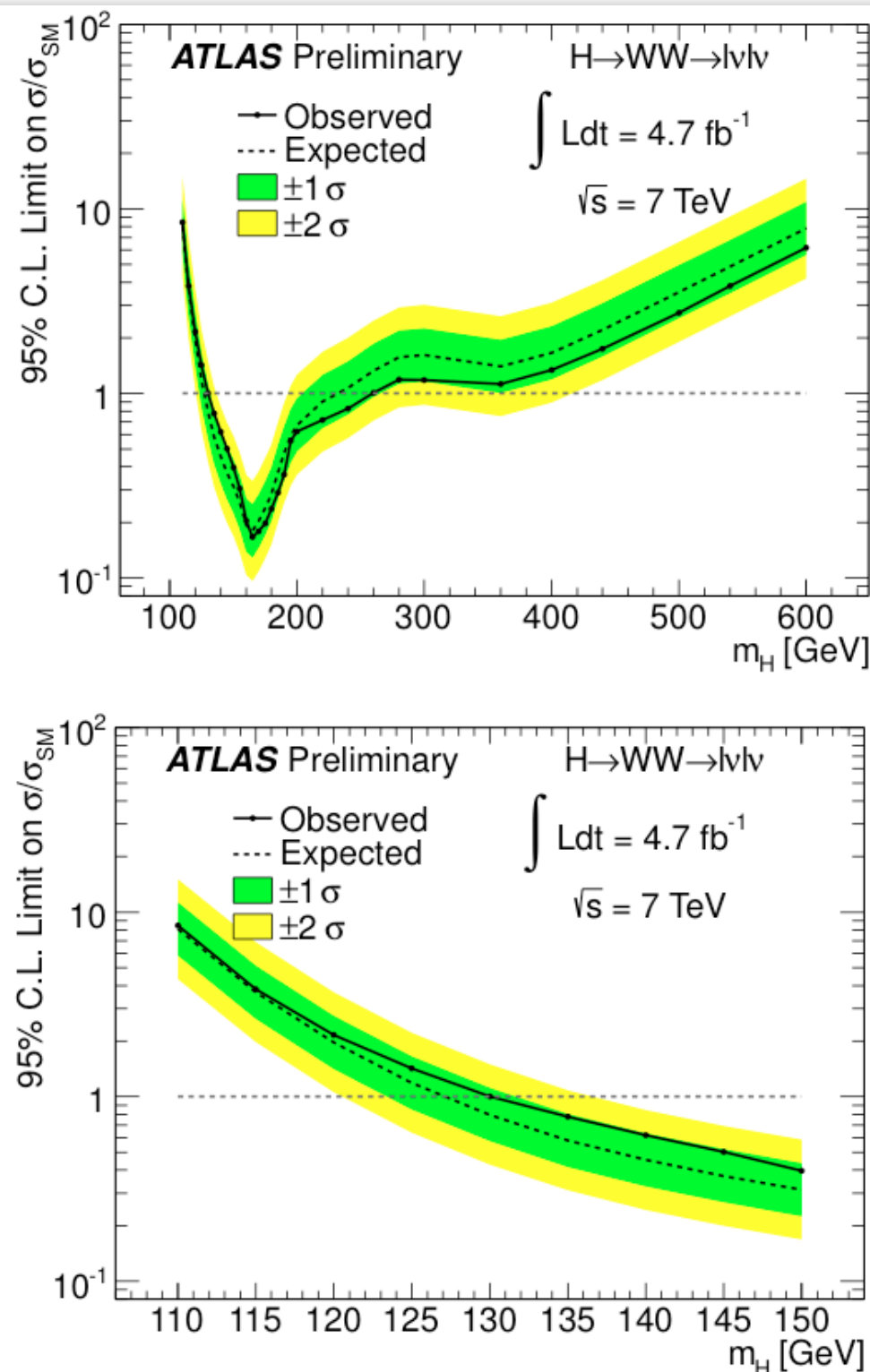
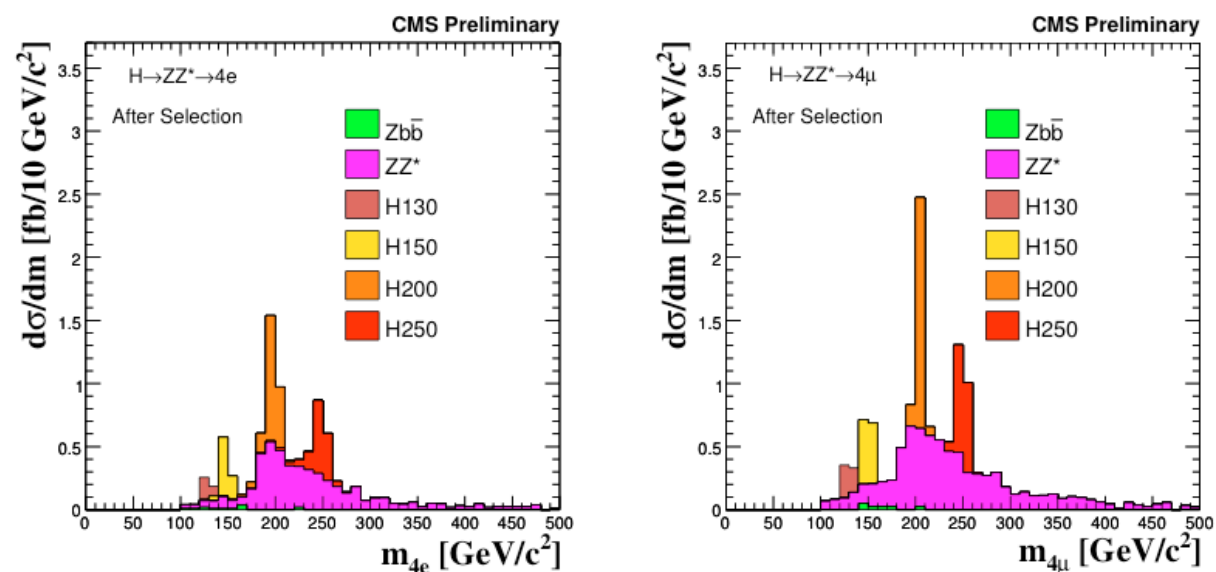


Figure 6: Expected (dashed) and observed (solid) 95% CL upper limits on the cross section, normalised to the SM cross section, as a function of  $m_H$ , over the full mass range considered in this analysis (top) and restricted to the range  $m_H < 150$  GeV (bottom). The green and yellow regions indicate the  $\pm 1\sigma$  and  $\pm 2\sigma$  uncertainty bands on the expected limit, respectively. The results at neighbouring mass points are highly correlated due to the limited mass resolution in this final state.

## ZZ searches—the ingredients

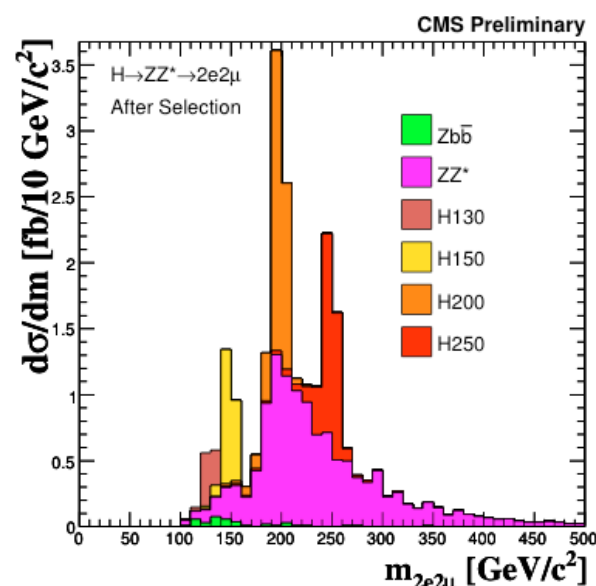
- *Select four ~isolated leptons*
  - *Very clean—this already suppresses most backgrounds to a negligible level*
  - *Remaining backgrounds are “irreducible” continuum ZZ (leading source of real four-high- $p_T$ -lepton events in the SM) and Z+jets, top, Zbb (leading sources of  $<4$  real lepton +  $\geq 1$  fake leptons)*
  - *Many leptons  $\Rightarrow$  keep acceptance, reconstruction and identification (isolation) efficiencies high*
  - *$M_H < 160$  GeV  $\Rightarrow$  ZZ\*  $\Rightarrow$  one of the four leptons is often very low  $p_T$  (e.g. CMS takes  $p_T > 7/5$  GeV for e/ $\mu$ )*
- *Backgrounds*
  - *SM ZZ from simulation, high  $M_{lll}$  control region*
  - *Non-ZZ (e.g. fake lepton) backgrounds from data-driven fakeable object method / SS control regions*
- *Example: CMS selection*
  - *$|\eta| < 2.5/2.4$  (e/ $\mu$ )*
  - *Track isolation/ $p_T < 0.7$  (in 0.3 cone)*
  - *On-shell Z:  $p_T^1 > 20$  GeV,  $p_T^2 > 10$  GeV,  $50 < m_{ll} < 120$  GeV*
  - *Off-shell Z:  $m_{ll} > 12$  GeV*
  - *$m_{lll} > 100$  GeV*
  - *+ tighter constraints on impact param. and sum of relative calo. and track isolation for lepton pairs.*
  - *+ charge/flavor requirements where appropriate*

# ZZ mode—early estimated sensitivity



(a)

(b)



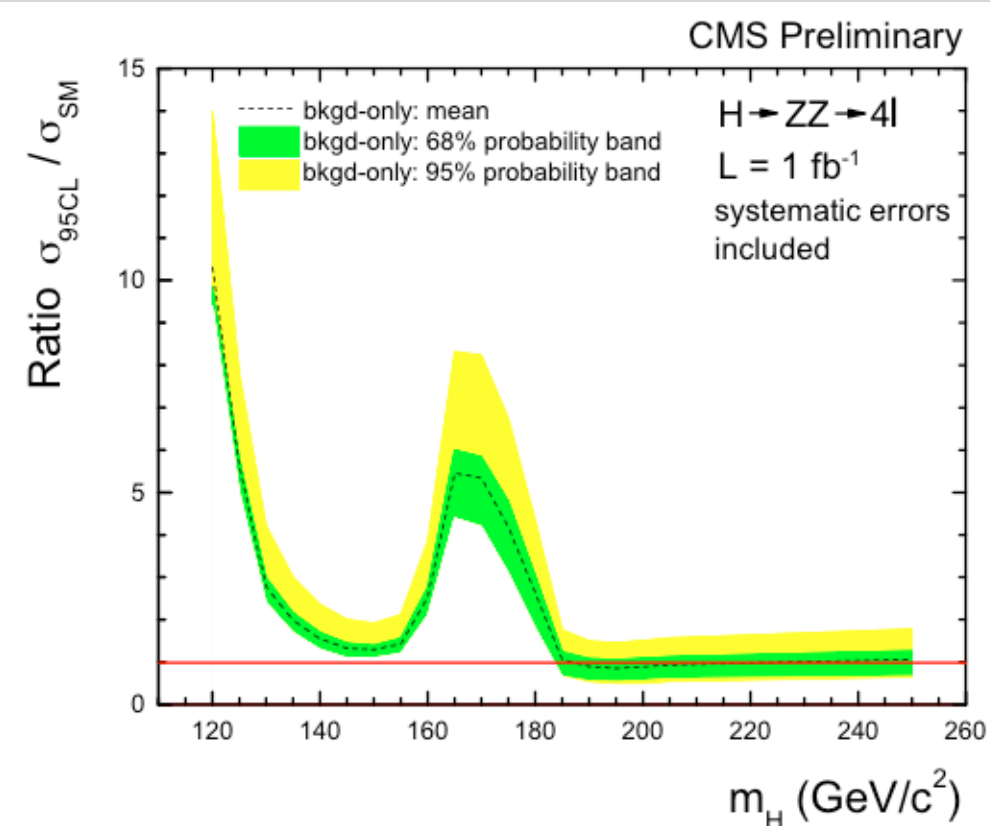
(c)

Figure 7: Four lepton invariant mass differential cross section after baseline selection for (a) 4e, (b) 4μ and (c) 2e2μ channel.

CMS PAS HIG-08-003 (1/fb, 14 TeV)

$m_H$ ( $\text{GeV}/c^2$ )	Events at $1 \text{ fb}^{-1}$		Significance	$R_{95\% \text{ C.L.}}$
	$N_{s+b}$	$N_b$		
120	0.52	0.19	0.13	10.3
130	1.56	0.29	1.32	2.79
140	2.85	0.42	2.22	1.55
150	3.52	0.47	2.64	1.29
160	1.98	0.47	1.36	2.53
170	1.34	0.61	0.50	5.35
180	3.16	1.38	1.09	2.64
190	9.24	2.74	2.92	0.89
200	10.6	3.52	2.87	0.89
250	8.02	2.66	2.49	1.06

Table 3: Expected significance and expected values of  $R_{95\% \text{ C.L.}}$  for selected Higgs boson masses.





# ZZ mode—early estimated sensitivity

ATL-PHYS-PUB-2010-009

$M_H(\text{GeV})$	120	130	140	150	165	170	180	190
SM ZZ	0.090	0.094	0.083	0.089	0.121	0.147	0.376	0.981
top & Z+jets	0.005	0.004	0.005	0.004	0.005	0.005	0.003	0.003
Total background	0.095	0.098	0.088	0.093	0.126	0.152	0.379	0.984
Signal	0.105	0.319	0.595	0.713	0.185	0.192	0.458	1.49
$M_H(\text{GeV})$	200	220	240	260	300	400	500	600
SM ZZ	1.29	1.18	0.92	0.89	0.72	0.48	0.49	0.39
Signal	1.60	1.46	1.25	1.08	0.88	0.67	0.29	0.13

Table 11: Estimated number of events in the signal region for the signal and the major backgrounds at an integrated luminosity of  $1 \text{ fb}^{-1}$  for  $\sqrt{s} = 7 \text{ TeV}$  after the full event selection in  $H \rightarrow ZZ \rightarrow 4l$  (the  $4e$ ,  $2e2\mu$  and the  $4\mu$  final states are summed) .

ATL-PHYS-PUB-2010-009

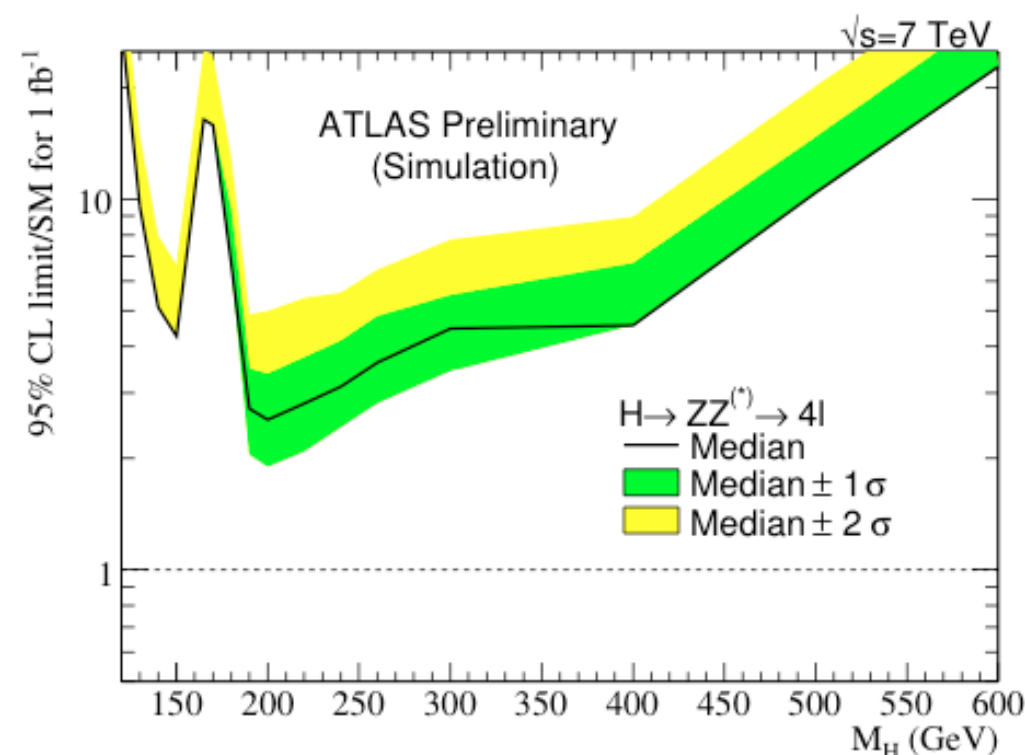


Figure 10: Expected 95% CL upper limits on the Standard Model Higgs boson production in the  $H \rightarrow ZZ^{(*)} \rightarrow 4l$  channel as a function of the Higgs mass, for the 7 TeV centre-of-mass energy. The bands indicate the range in which we expect the limit will lie, depending upon the data. These limits were obtained with the  $CL_s$  method used in LEP and Tevatron experiments [35].

# ZZ searches—results

arXiv:1202.1997

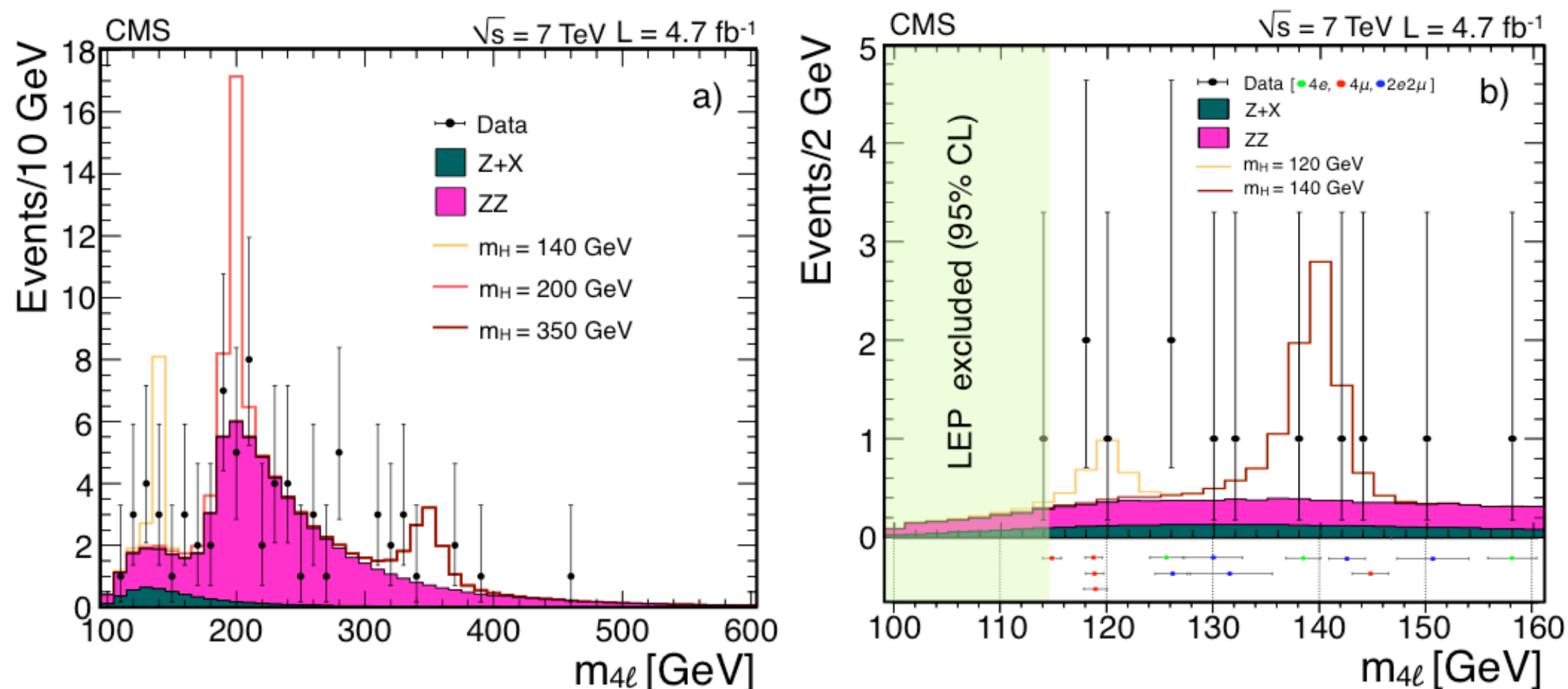


Figure 1: a) Distribution of the four-lepton reconstructed mass for the sum of the  $4e$ ,  $4\mu$ , and  $2e2\mu$  channels. b) Expansion of the low mass range with existing exclusion limits at 95% CL; also shown are the central values and individual candidate mass measurement uncertainties. Points represent the data, shaded histograms represent the background and unshaded histogram the signal expectations.

## ZZ searches—results

CMS, arXiv:1202.1997

Table 1: The number of candidates observed, compared to background and signal rates for each final state for  $100 < m_{4\ell} < 600$  GeV for the baseline selection. For the Z+X background, the estimations are based on data

Channel	4e	4 $\mu$	2e2 $\mu$
ZZ background	$12.27 \pm 1.16$	$19.11 \pm 1.75$	$30.25 \pm 2.78$
Z+X	$1.67 \pm 0.55$	$1.13 \pm 0.55$	$2.71 \pm 0.96$
All background	$13.94 \pm 1.28$	$20.24 \pm 1.83$	$32.96 \pm 2.94$
$m_H = 120$ GeV	0.25	0.62	0.68
$m_H = 140$ GeV	1.32	2.48	3.37
$m_H = 350$ GeV	1.95	2.61	4.64
Observed	12	23	37

Recall: CMS PAS HIG-08-003 (1/fb, 14 TeV)

$m_H$ (GeV/ $c^2$ )	Events at 1 fb $^{-1}$		Significance	$R_{95\% \text{ C.L.}}$
	$N_{s+b}$	$N_b$		
120	0.52	0.19	0.13	10.3
130	1.56	0.29	1.32	2.79
140	2.85	0.42	2.22	1.55
150	3.52	0.47	2.64	1.29
160	1.98	0.47	1.36	2.53
170	1.34	0.61	0.50	5.35
180	3.16	1.38	1.09	2.64
190	9.24	2.74	2.92	0.89
200	10.6	3.52	2.87	0.89
250	8.02	2.66	2.49	1.06

## ZZ searches—results

ATLAS, arXiv:1202.1415

Table 3: The expected numbers of background events, with their systematic uncertainty, separated into “Low- $m_{4\ell}$ ” ( $m_{4\ell} < 180$  GeV) and “High- $m_{4\ell}$ ” ( $m_{4\ell} \geq 180$  GeV) regions, compared to the observed numbers of events. The expectations for a Higgs boson signal for five different  $m_H$  values are also given.

	$\mu^+\mu^-\mu^+\mu^-$		$e^+e^-\mu^+\mu^-$		$e^+e^-e^+e^-$	
	Low- $m_{4\ell}$	High- $m_{4\ell}$	Low- $m_{4\ell}$	High- $m_{4\ell}$	Low- $m_{4\ell}$	High- $m_{4\ell}$
Int. Luminosity	4.8 fb $^{-1}$		4.8 fb $^{-1}$		4.9 fb $^{-1}$	
$ZZ^{(*)}$	$2.1 \pm 0.3$	$16.3 \pm 2.4$	$2.8 \pm 0.6$	$25.2 \pm 3.8$	$1.2 \pm 0.3$	$10.4 \pm 1.5$
$Z + \text{jets and } t\bar{t}$	$0.16 \pm 0.06$	$0.02 \pm 0.01$	$1.4 \pm 0.5$	$0.17 \pm 0.08$	$1.6 \pm 0.7$	$0.18 \pm 0.08$
Total Background	$2.2 \pm 0.3$	$16.3 \pm 2.4$	$4.3 \pm 0.8$	$25.4 \pm 3.8$	$2.8 \pm 0.8$	$10.6 \pm 1.5$
Data	3	21	3	27	2	15
$m_H = 130$ GeV	$1.00 \pm 0.17$		$1.22 \pm 0.21$		$0.43 \pm 0.08$	
$m_H = 150$ GeV	$2.1 \pm 0.4$		$2.9 \pm 0.4$		$1.12 \pm 0.18$	
$m_H = 200$ GeV	$4.9 \pm 0.7$		$7.7 \pm 1.0$		$3.1 \pm 0.4$	
$m_H = 400$ GeV	$2.0 \pm 0.3$		$3.3 \pm 0.5$		$1.49 \pm 0.21$	
$m_H = 600$ GeV	$0.34 \pm 0.04$		$0.62 \pm 0.10$		$0.30 \pm 0.06$	

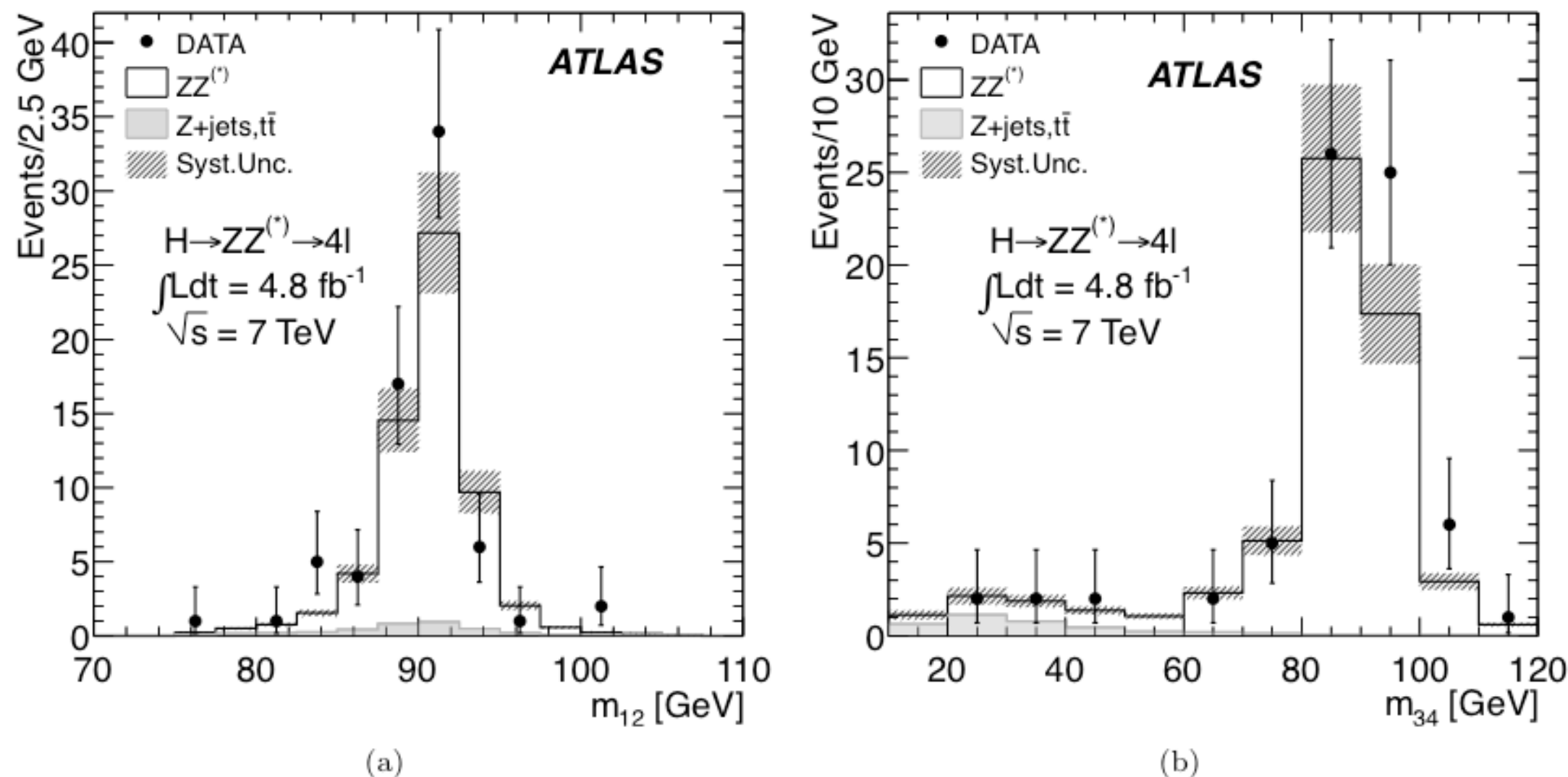


Figure 3: Invariant mass distributions (a)  $m_{12}$  and (b)  $m_{34}$  for the selected candidates. The data (dots) are compared to the background expectations from the dominant  $ZZ^{(*)}$  process and the sum of  $t\bar{t}$ ,  $Zb\bar{b}$  and  $Z$  + light jets processes. Error bars represent 68.3% central confidence intervals.

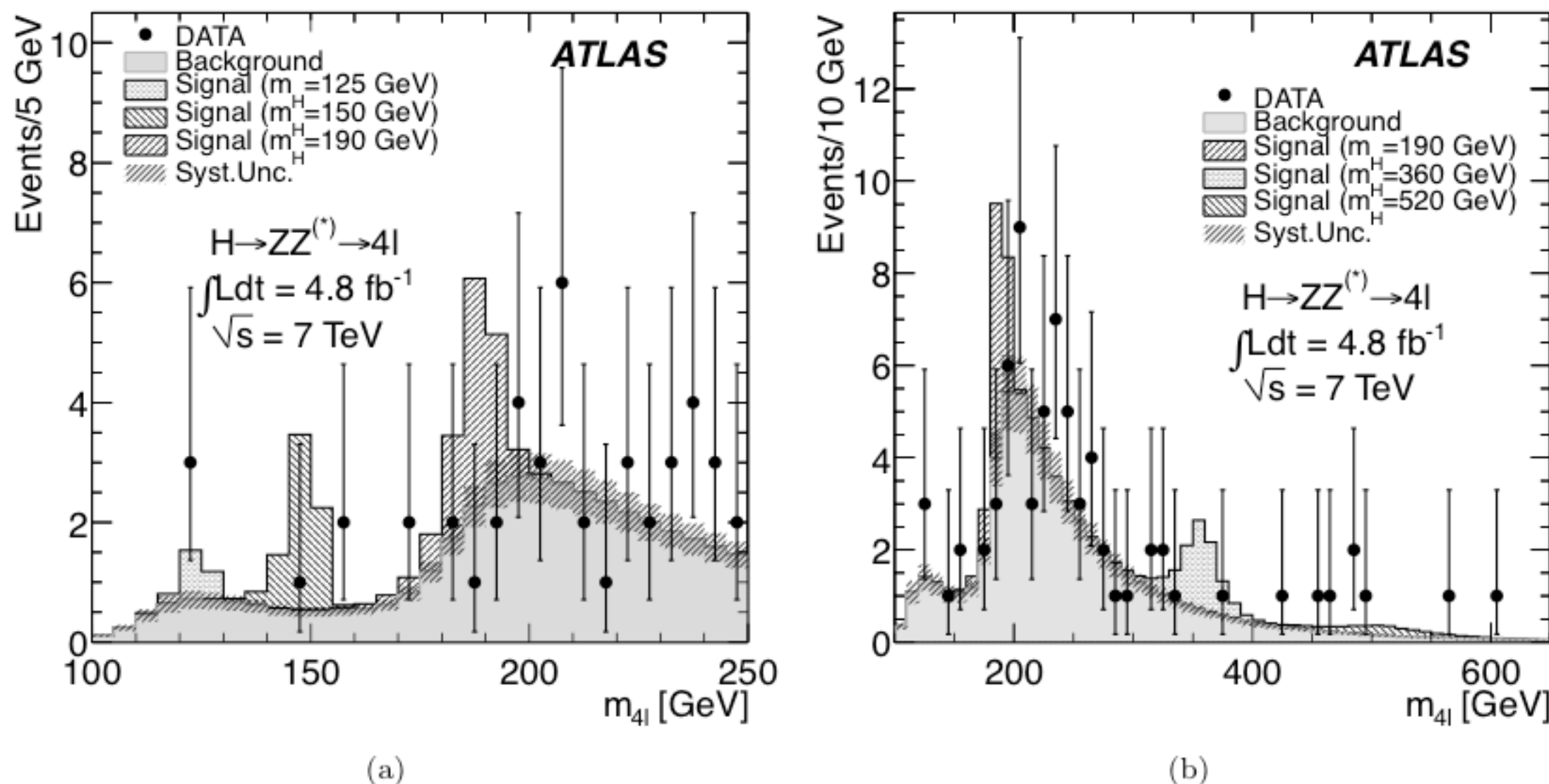


Figure 4:  $m_{4\ell}$  distribution of the selected candidates, compared to the background expectation for (a) the 100 – 250 GeV mass range and (b) the full mass range of the analysis. Error bars represent 68.3% central confidence intervals. The signal expectation for several  $m_H$  hypotheses is also shown. The resolution of the reconstructed Higgs mass is dominated by detector resolution at low  $m_H$  values and by the Higgs boson width at high  $m_H$ .



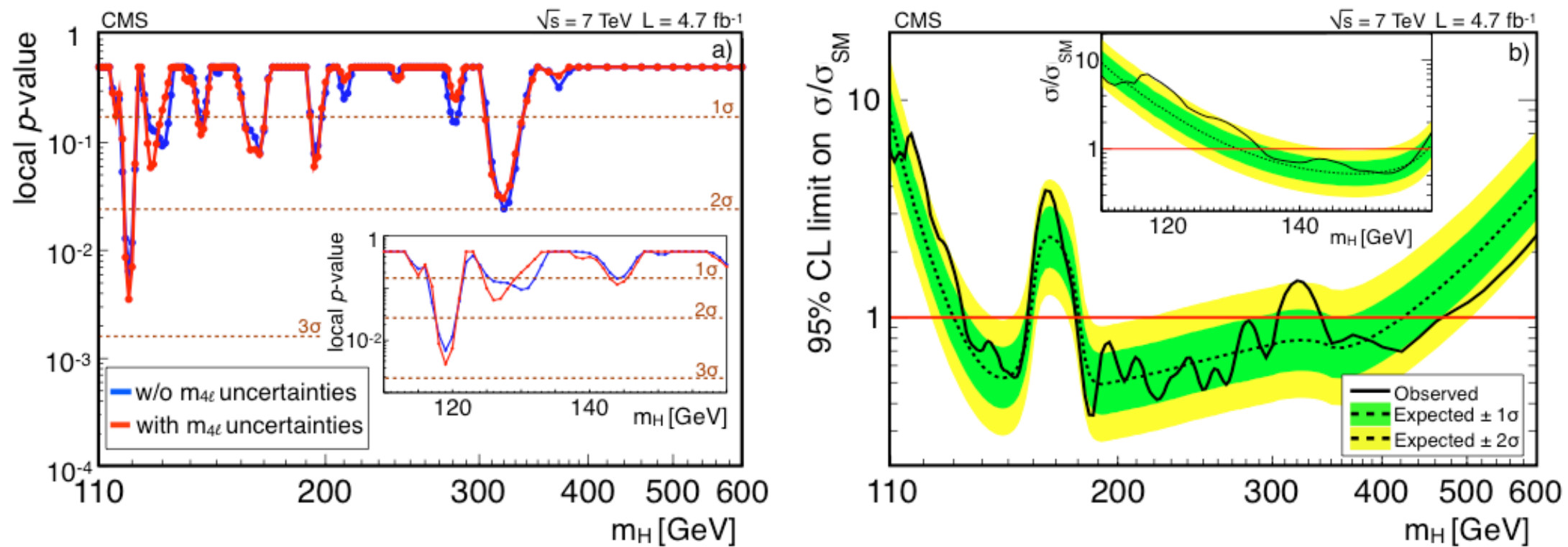


Figure 2: a) The significance of the local excesses with respect to the standard model expectation as a function of the Higgs boson mass, without (blue) or with (red) individual candidate mass measurement uncertainties. b) The observed and the median expected upper limits at 95% CL on  $\sigma(\text{pp} \rightarrow \text{H} + \text{X}) \times \mathcal{B}(\text{ZZ} \rightarrow 4\ell)$ , normalized to the standard model cross section values  $\sigma_{\text{SM}}$ , for a Higgs boson in the mass range 110–600 GeV, using the  $\text{CL}_s$  approach. The insets expand the low mass range.

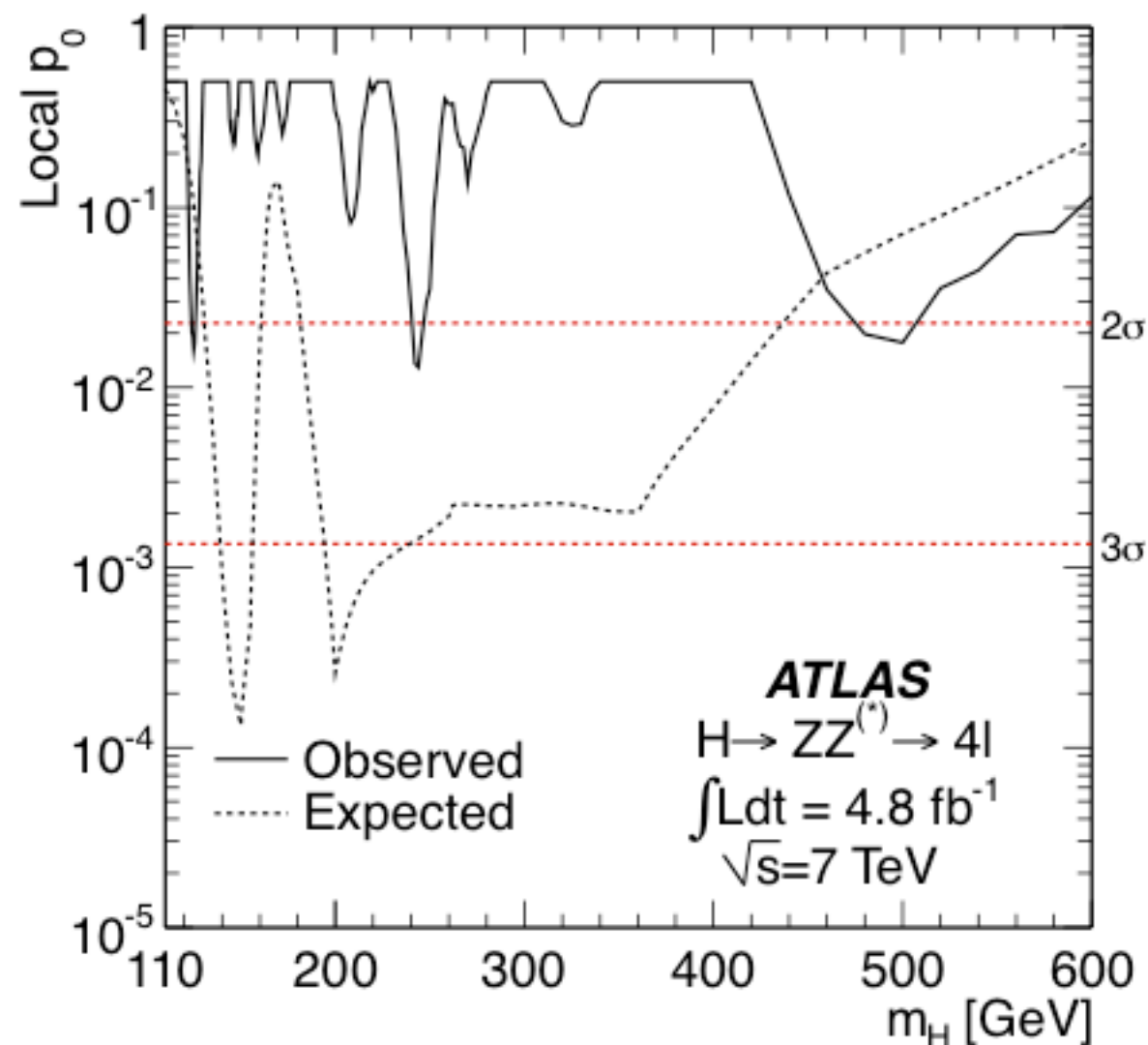


Figure 6: The observed local  $p_0$ , the probability that the background fluctuates to the observed number of events or higher, is shown as the solid line. The dashed curve shows the expected median local  $p_0$  for the signal hypothesis when tested at  $m_H$ . The two horizontal dashed lines indicate the  $p_0$  values corresponding to local significances of  $2\sigma$  and  $3\sigma$ .

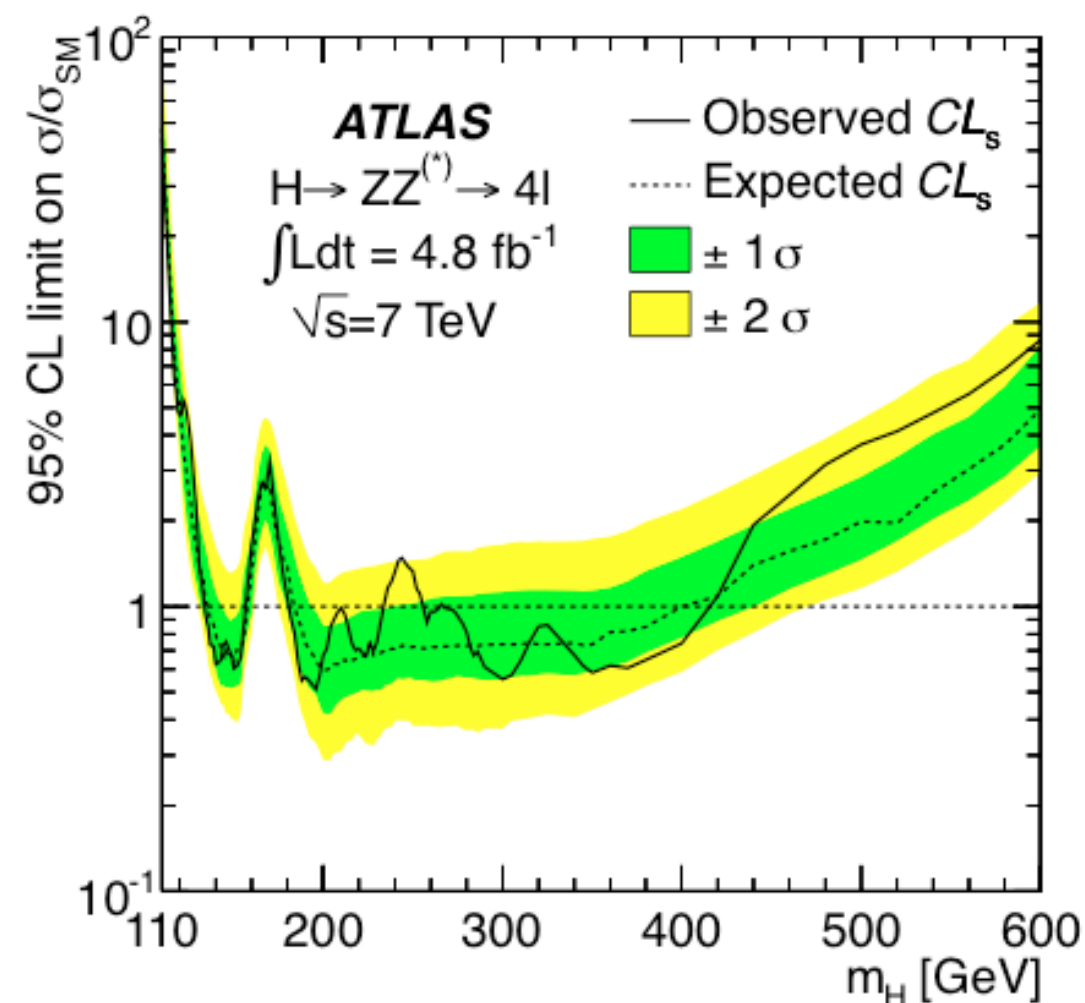


Figure 5: The expected (dashed) and observed (full line) 95% CL upper limits on the Standard Model Higgs boson production cross section as a function of  $m_H$ , divided by the expected SM Higgs boson cross section. The dark (green) and light (yellow) bands indicate the expected limits with  $\pm 1\sigma$  and  $\pm 2\sigma$  fluctuations, respectively.



# What to conclude?

- Small excess in **ZZ** is consistent both with a statistical fluctuation or (to a lesser extent) a signal
- Nothing to even call an excess in **WW**

ATL-PHYS-CONF-2012-019

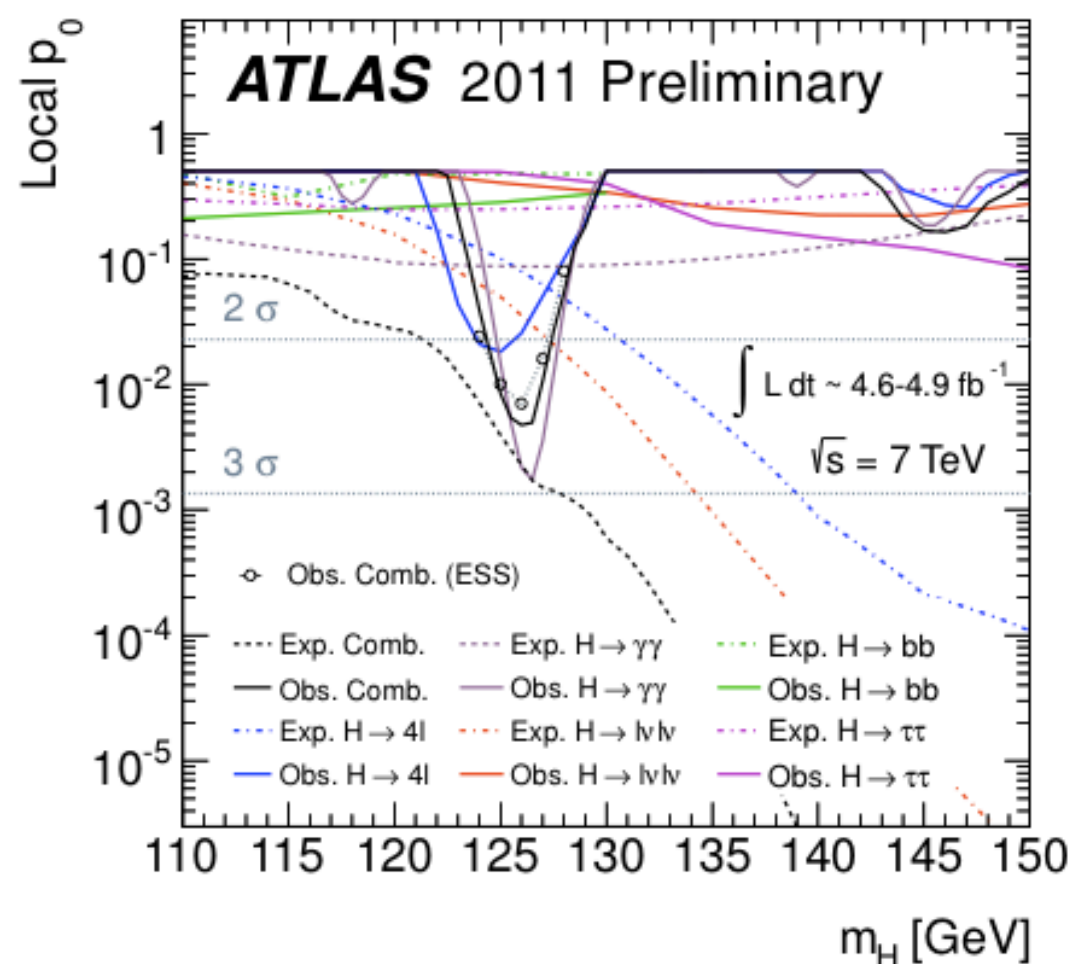


Figure 5: The local probability  $p_0$  for a background-only experiment to be more signal-like than the observation, for individual channels and the combination. The full curves give the observed individual and combined  $p_0$ . The dashed curves show the median expected value under the hypothesis of a SM Higgs boson signal at that mass. The two horizontal dashed lines indicate the  $p_0$  corresponding to significances of  $2\sigma$  and  $3\sigma$ . The points indicate the combined observed local  $p_0$  estimated using ensemble tests and taking into account energy scale systematic uncertainties (ESS).

## What next?

- *Can I predict what we'll see with  $\sim 15/\text{fb}$  of new 8 TeV data?*
  - *No—signal could grow or go away, tension in diphoton and ZZ vs WW could increase or decrease*
- *Sensitivity will change*
  - *e.g.  $H \rightarrow WW$  cross section will increase faster than continuum WW, slower than  $t\bar{t}$*
  - *Increased pile-up may require new techniques to keep its effects under control (e.g. DY bkg. to WW)*
  - *Analysis improvements (e.g. more widespread use of MVAs, additional channels, reduced systematics)*

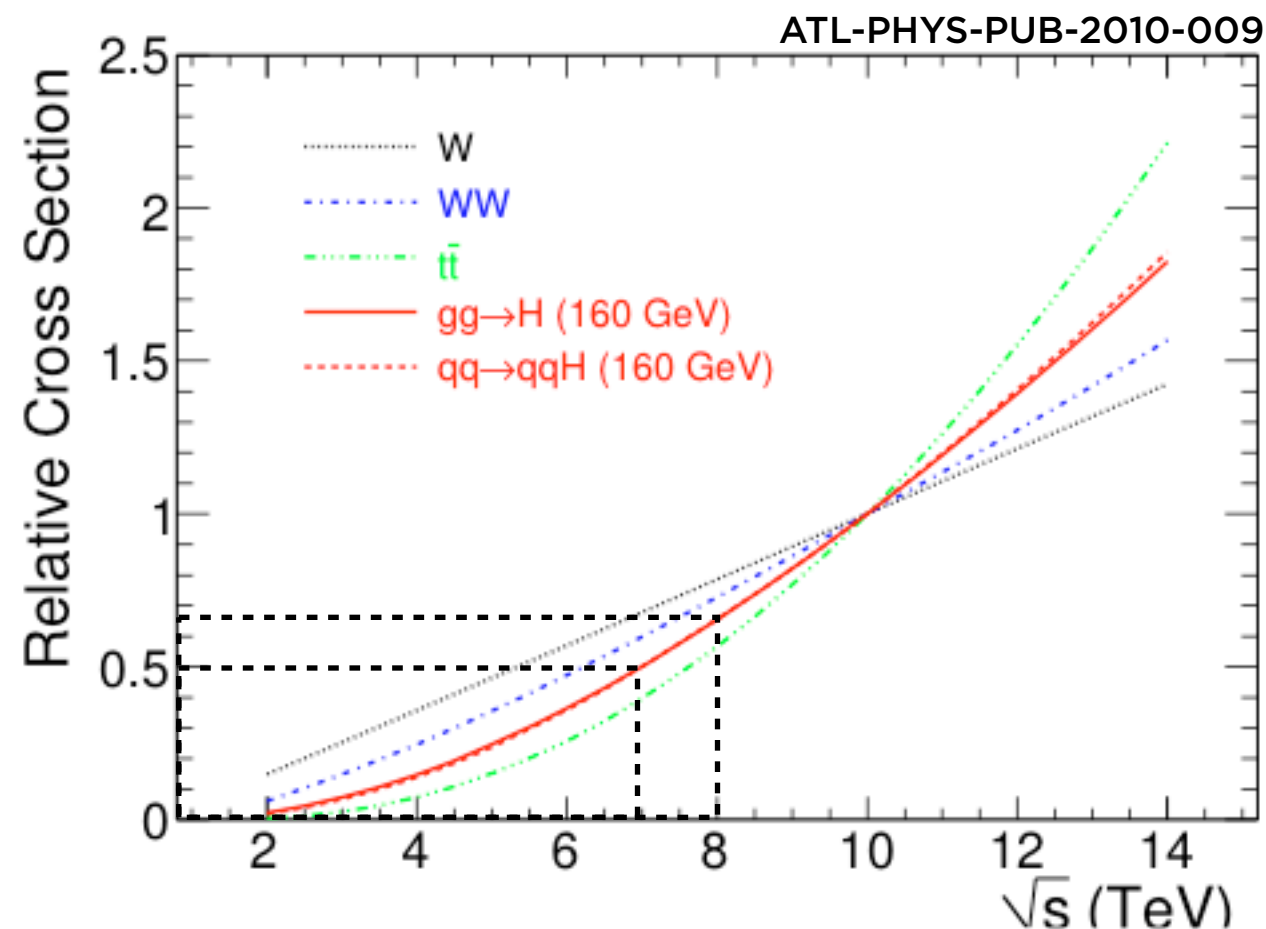


Figure 3: Relative NLO cross-sections from MCFM [12] as functions of  $\sqrt{s}$  for the signal ( $M_H = 160$  GeV) and main background processes.

# How did the sensitivity projections do?

- *ATLAS ZZ: projected ~0.5 bkg + 1.5 signal at 130 GeV, vs. 9.3 bkg + 2.65 signal actual.*

ATLAS, arXiv:1202.1415

Table 3: The expected numbers of background events, with their systematic uncertainty, separated into “Low- $m_{4\ell}$ ” ( $m_{4\ell} < 180$  GeV) and “High- $m_{4\ell}$ ” ( $m_{4\ell} \geq 180$  GeV) regions, compared to the observed numbers of events. The expectations for a Higgs boson signal for five different  $m_H$  values are also given.

	$\mu^+\mu^-\mu^+\mu^-$		$e^+e^-\mu^+\mu^-$		$e^+e^-e^+e^-$	
	Low- $m_{4\ell}$	High- $m_{4\ell}$	Low- $m_{4\ell}$	High- $m_{4\ell}$	Low- $m_{4\ell}$	High- $m_{4\ell}$
Int. Luminosity	4.8 fb <sup>-1</sup>		4.8 fb <sup>-1</sup>		4.9 fb <sup>-1</sup>	
$ZZ^{(*)}$	2.1 ± 0.3	16.3 ± 2.4	2.8 ± 0.6	25.2 ± 3.8	1.2 ± 0.3	10.4 ± 1.5
$Z + \text{jets and } t\bar{t}$	0.16 ± 0.06	0.02 ± 0.01	1.4 ± 0.5	0.17 ± 0.08	1.6 ± 0.7	0.18 ± 0.08
Total Background	2.2 ± 0.3	16.3 ± 2.4	4.3 ± 0.8	25.4 ± 3.8	2.8 ± 0.8	10.6 ± 1.5
Data	3	21	3	27	2	15
$m_H = 130$ GeV	1.00 ± 0.17		1.22 ± 0.21		0.43 ± 0.08	
$m_H = 150$ GeV	2.1 ± 0.4		2.9 ± 0.4		1.12 ± 0.18	
$m_H = 200$ GeV	4.9 ± 0.7		7.7 ± 1.0		3.1 ± 0.4	
$m_H = 400$ GeV	2.0 ± 0.3		3.3 ± 0.5		1.40 ± 0.21	
$m_H =$						

ATL-PHYS-PUB-2010-009

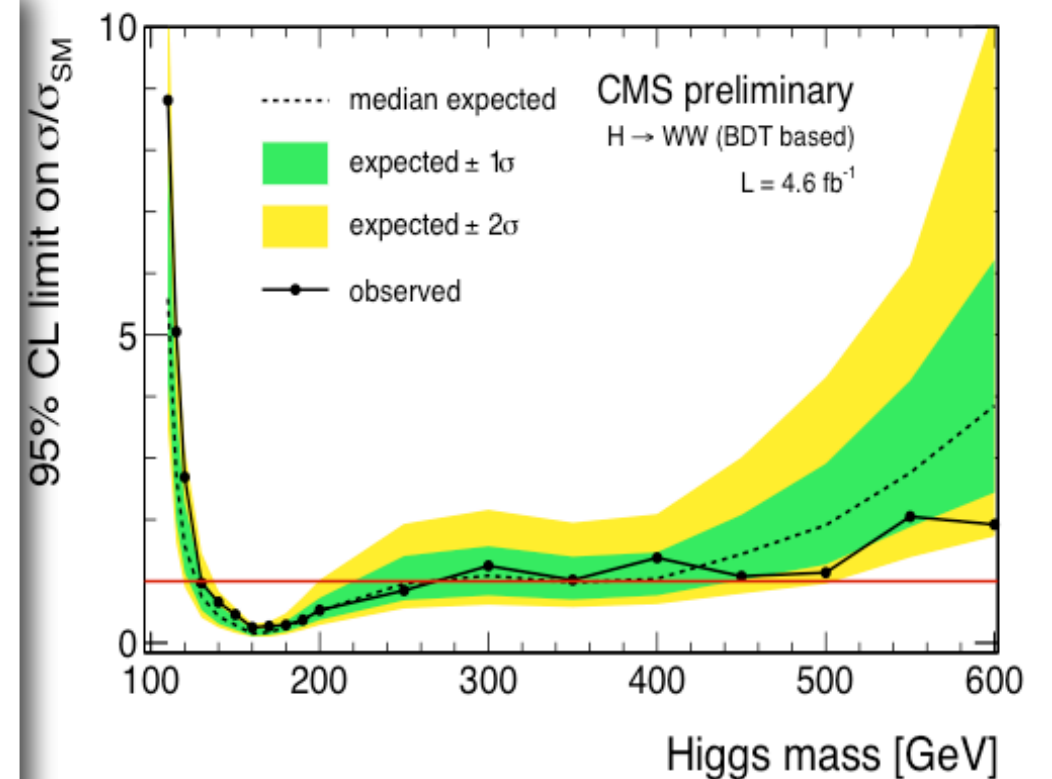
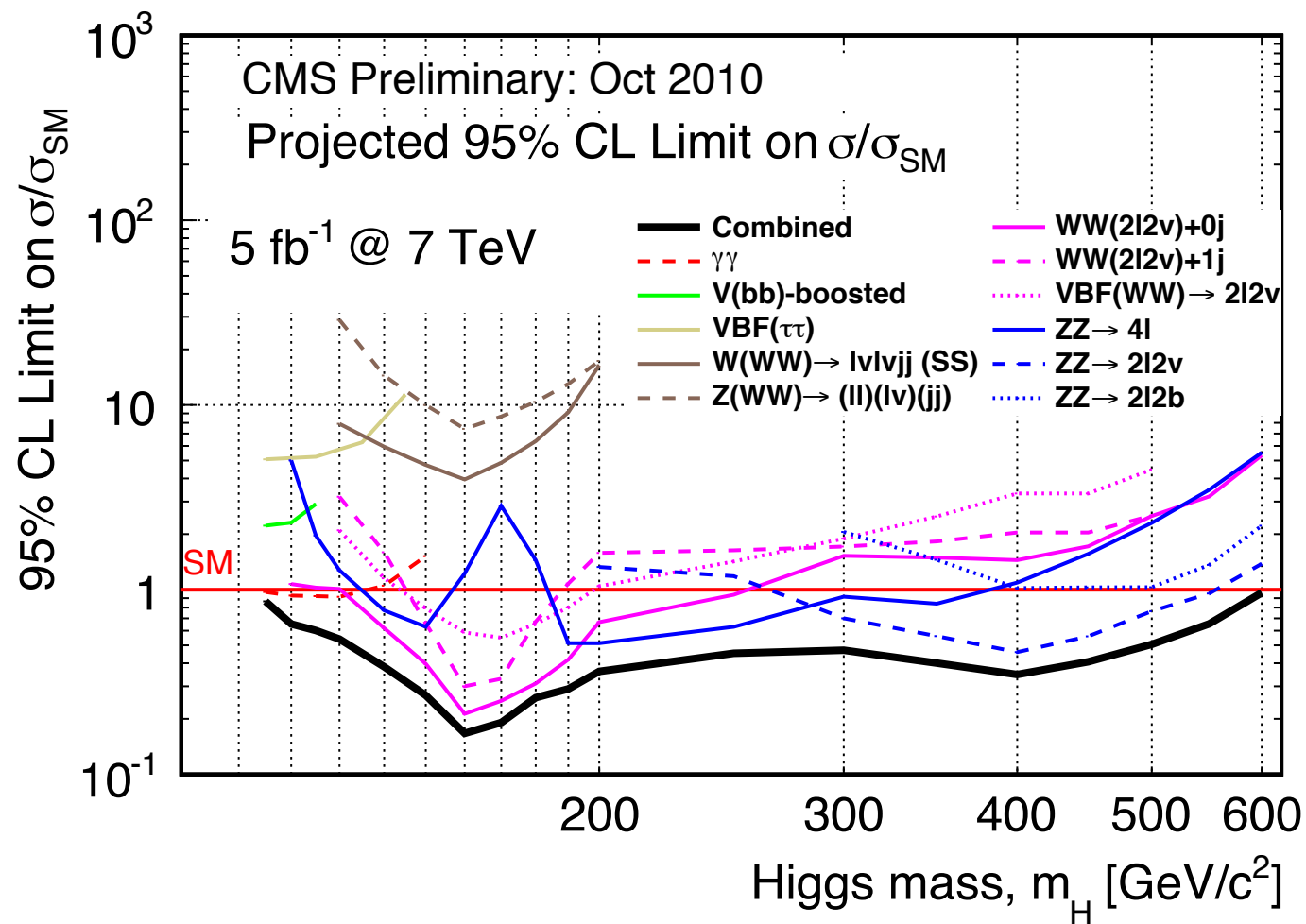
$M_H(\text{GeV})$	120	130	140	150	165	170	180	190
SM ZZ	0.090	0.094	0.083	0.089	0.121	0.147	0.376	0.981
top & Z+jets	0.005	0.004	0.005	0.004	0.005	0.005	0.003	0.003
Total background	0.095	0.098	0.088	0.093	0.126	0.152	0.379	0.984
Signal	0.105	0.319	0.595	0.713	0.185	0.192	0.458	1.49
$M_H(\text{GeV})$	200	220	240	260	300	400	500	600
SM ZZ	1.29	1.18	0.92	0.89	0.72	0.48	0.49	0.39
Signal	1.60	1.46	1.25	1.08	0.88	0.67	0.29	0.13

Table 11: Estimated number of events in the signal region for the signal and the major backgrounds at an integrated luminosity of 1 fb<sup>-1</sup> for  $\sqrt{s} = 7$  TeV after the full event selection in  $H \rightarrow ZZ \rightarrow 4l$  (the  $4e$ ,  $2e2\mu$  and the  $4\mu$  final states are summed) .

## How did the sensitivity projections do?

- Example: CMS WW: projected  $m_H < 130$  GeV vs  $< 127$  GeV actual; projected  $\sim 1 \times \text{SM}$  at 130 GeV  $0.7 \times \text{SM}$  in finished analysis

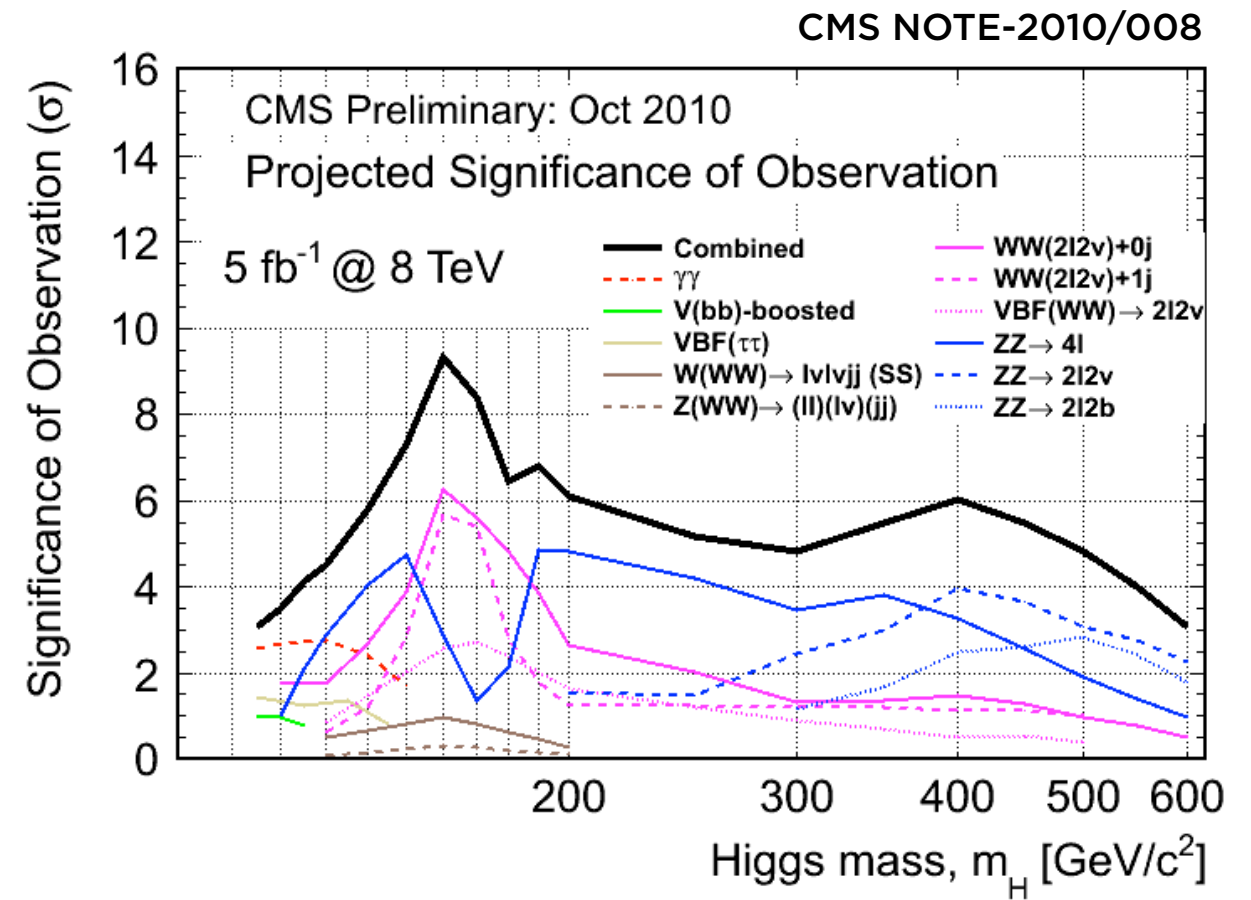
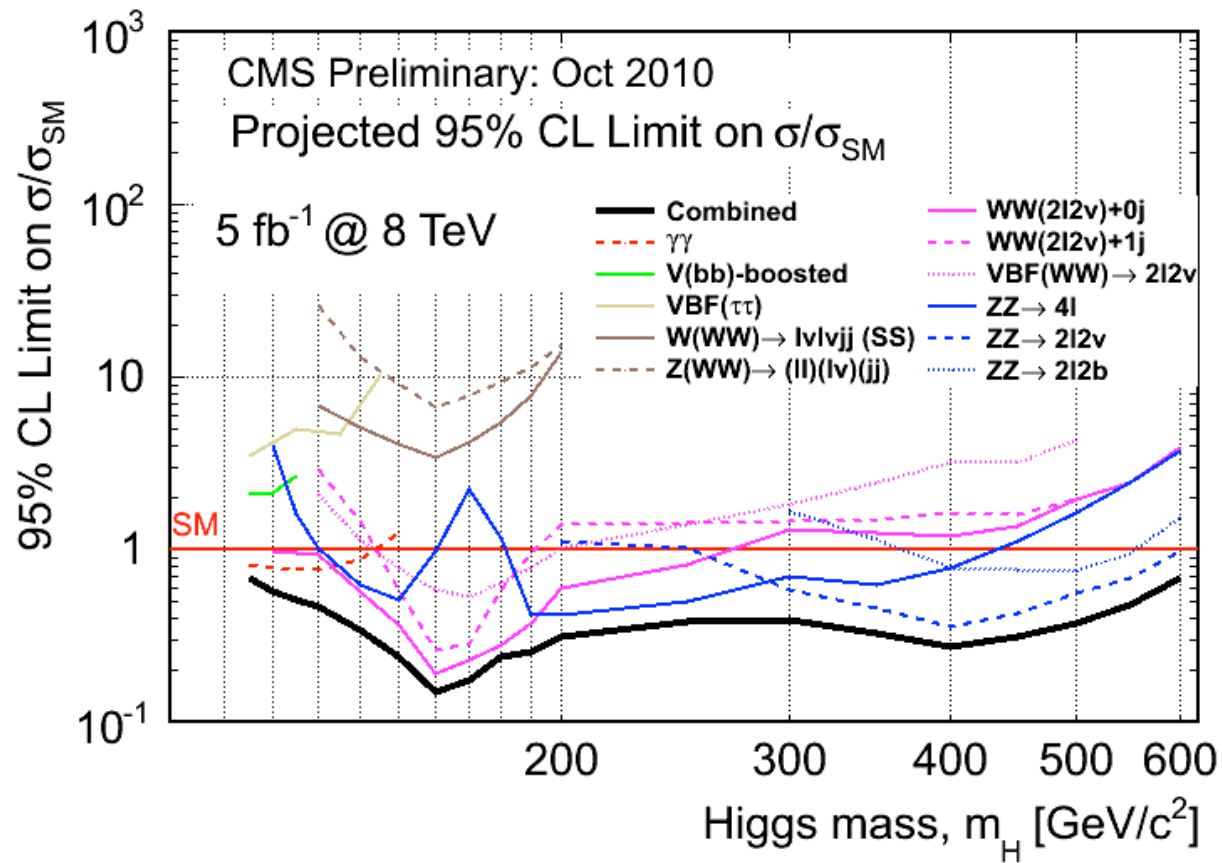
CMS NOTE-2010/008



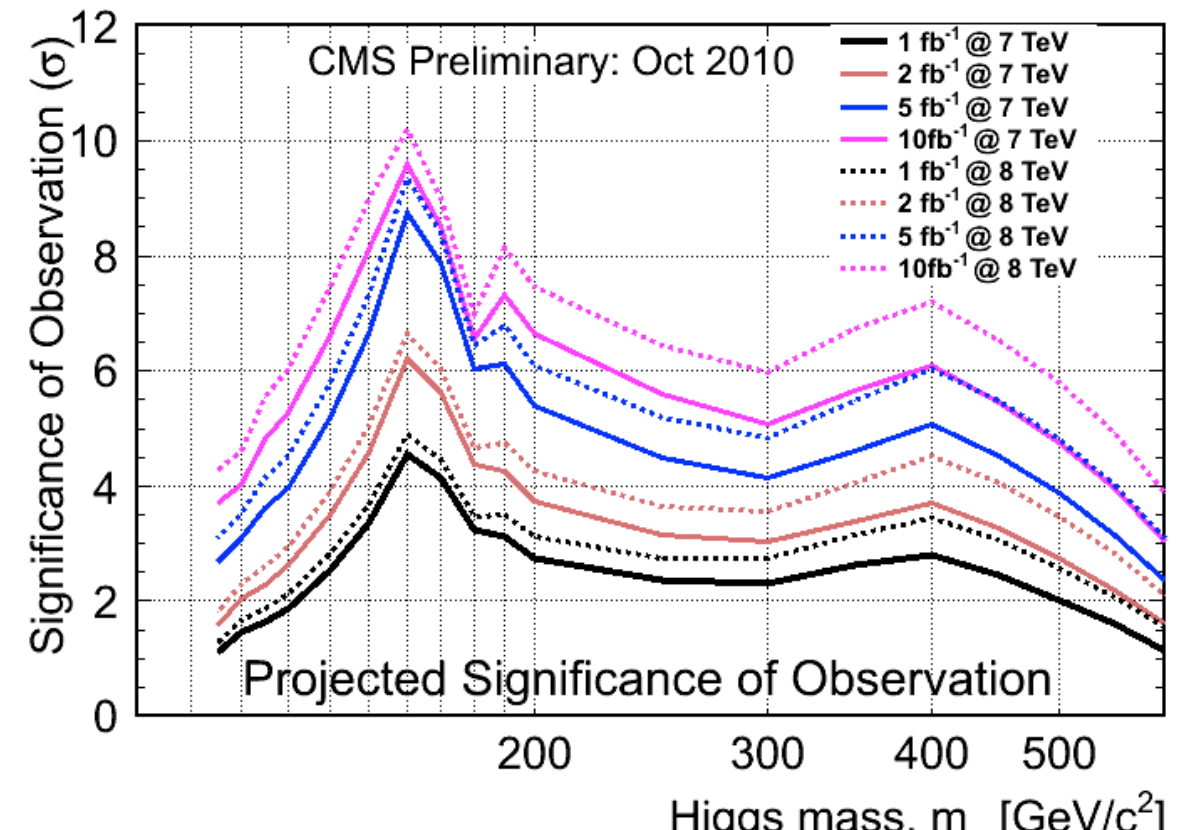
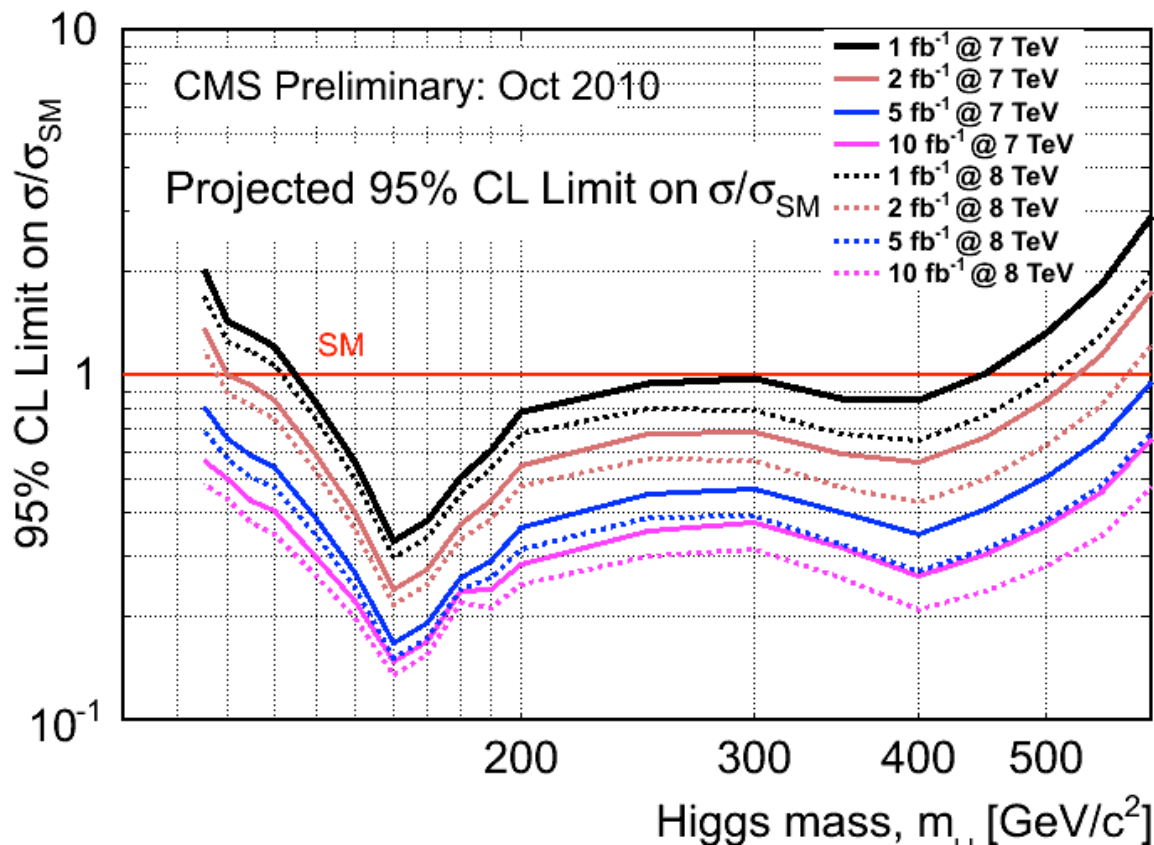
(b)

per limits on the cross section times branching  
to the SM value using cut-based (a) and multi-  
obtained using the CLs approach.

# What to expect for 8 TeV?



- 8 TeV predictions very similar to 7 TeV for WW, marginally better for ZZ
- Could exclude down past 0.1 SM at 160 GeV; expect >5 sigma significance for  $m_H > 120$  GeV(?)

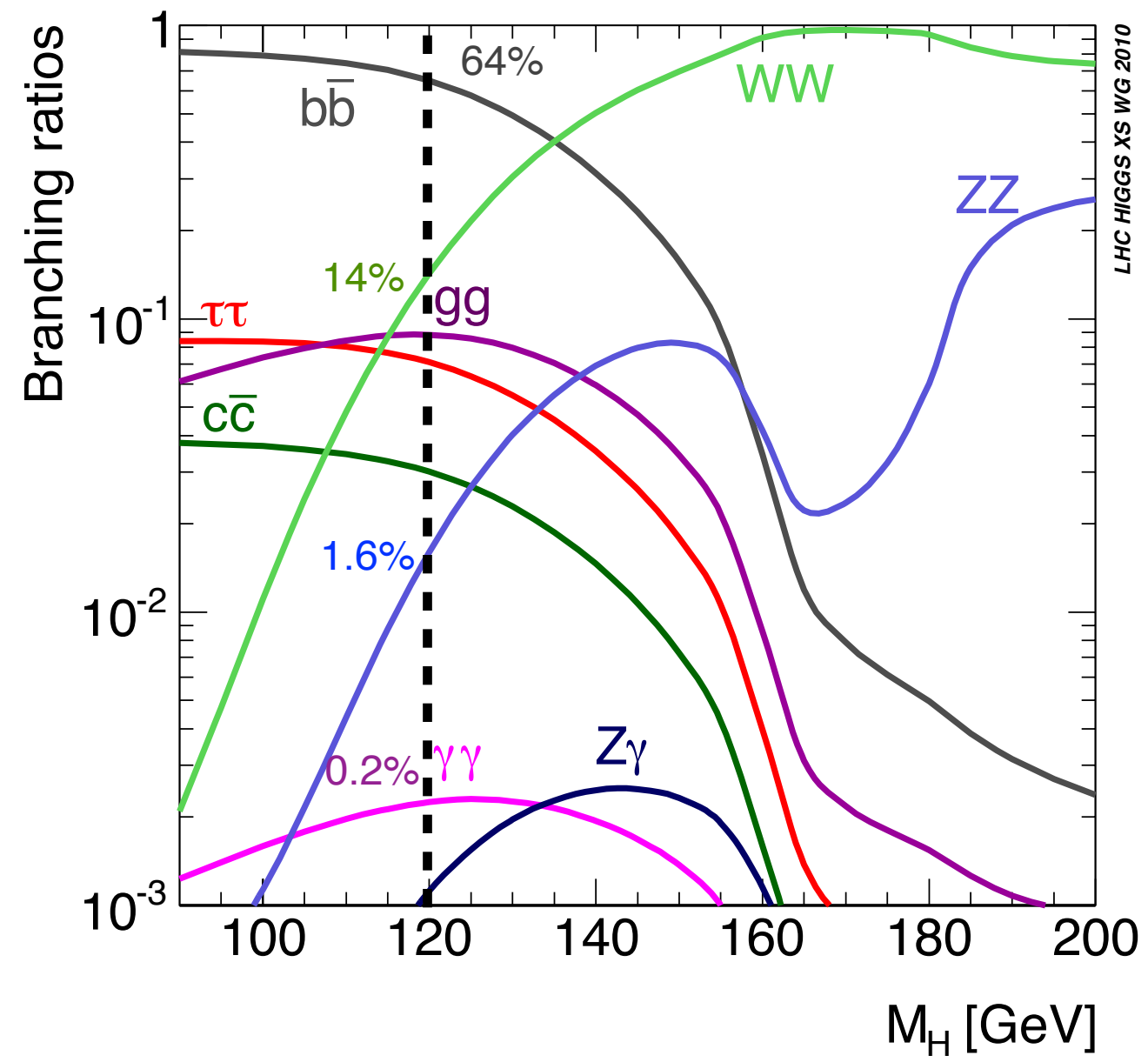




# Summary

- *Hints, but no reliable evidence for a Higgs in the  $WW$  or  $ZZ$  decay modes*
  - *Large swath of high mass excluded at nominal cross sections*
  - *(ATLAS and CMS full combinations suggest  $\sim 115\text{--}130$  GeV or bust)*
- *The low mass  $WW \rightarrow ll$  analysis is very tricky—requires accurate understanding of normalization of  $WW$ ,  $DY$ ,  $W+\text{jets}$ ,  $W\gamma$ ,  $W\gamma^*$* 
  - *Looking in tail kinematic regions of several backgrounds*
  - *Sensitivity projections suggest*
  - *If we see a signal in this channel, will we believe it?*
- *The  $ZZ \rightarrow 4l$  analysis will become more interesting this year, with (finally) more than a couple events expected.*
  - *(if tenuous signal is established, this illustrates that we'll have only a crude understanding of the branching ratios)*

# Additional Slides





## WW mode—Early estimated sensitivity

CMS NOTE 2006/047

Table 7: The expected number of events for an integrated luminosity of  $1 \text{ fb}^{-1}$  for the backgrounds. The relative efficiency with respect to the previous cut is given in parentheses. The last line shows the total selection efficiency together with the uncertainty from the limited Monte Carlo statistics.

<sup>1</sup> Note: For ggWW a jet veto is applied but its efficiency is conservatively scaled to 1 as this process is only known at LO [14].

	qq $\rightarrow$ WW	gg $\rightarrow$ WW	t $\bar{t}$	tWb	WZ	ZZ
$\sigma \times \text{BR}(e, \mu, \tau) [\text{fb}]$	11700	480	86200	3400	1630	1520
L1+HLT	6040 (52%)	286 (60%)	57380 (67%)	2320 (68%)	1062 (65%)	485 (32%)
2 lep, $ \eta  < 2$ , $p_t > 20 \text{ GeV}$ $\sigma_{\text{IP}} > 3$ , $ \Delta z_{\text{lep}}  < 0.2 \text{ cm}$	1398 (23%)	73 (26%)	15700 (27%)	676 (29%)	247 (23%)	163 (34%)
$E_t^{\text{miss}} > 50 \text{ GeV}$	646 (46%)	43 (59%)	9332 (59%)	391 (58%)	103 (42%)	70 (43%)
$\phi_{\ell\ell} < 45$	59 (9.2%)	11 (26%)	1649 (18%)	65 (17%)	14 (13%)	10 (15%)
$12 \text{ GeV} < m_{\ell\ell} < 40 \text{ GeV}$	29 (49%)	6.5 (57%)	661 (40%)	28 (43%)	1.8 (13%)	1.3 (12%)
Jet veto	23 (80%)	6.5 <sup>1</sup>	24 (3.6%)	3.6 (13%)	1.2 (70%)	0.98 (75%)
$30 \text{ GeV} < p_t^{\ell \text{ max}} < 55 \text{ GeV}$	17 (74%)	5.1 (78%)	13 (54%)	2.3 (63%)	0.85 (70%)	0.46 (47%)
$p_t^{\ell \text{ min}} > 25 \text{ GeV}$	12 (69%)	3.7 (73%)	9.8 (74%)	1.4 (62%)	0.50 (58%)	0.35 (76%)
$\varepsilon_{\text{tot}}$	$(0.103 \pm 0.008)\%$	$(0.77 \pm 0.04)\%$	$(0.011 \pm 0.002)\%$	$(0.041 \pm 0.005)\%$	$(0.031 \pm 0.006)\%$	$(0.023 \pm 0.006)\%$

## WW mode—Early estimated sensitivity

CMS NOTE 2006/047

Table 7: The expected number of events for an integrated luminosity of  $1 \text{ fb}^{-1}$  for the backgrounds. The relative efficiency with respect to the previous cut is given in parentheses. The last line shows the total selection efficiency together with the uncertainty from the limited Monte Carlo statistics.

<sup>1</sup> Note: For ggWW a jet veto is applied but its efficiency is conservatively scaled to 1 as this process is only known at LO [14].

	$qq \rightarrow WW$	$gg \rightarrow WW$	$t\bar{t}$	$tWb$	$WZ$	$ZZ$
$\sigma \times \text{BR}(e, \mu, \tau) [\text{fb}]$	11700	480	86200	3400	1630	1520
L1+HLT	6040 (52%)	286 (60%)	57380 (67%)	2320 (68%)	1062 (65%)	485 (32%)
2 lep, $ \eta  < 2$ , $p_t > 20 \text{ GeV}$ $\sigma_{\text{IP}} > 3$ , $ \Delta z_{\text{lep}}  < 0.2 \text{ cm}$	1398 (23%)	73 (26%)	15700 (27%)	676 (29%)	247 (23%)	163 (34%)
$E_t^{\text{miss}} > 50 \text{ GeV}$	646 (46%)	43 (59%)	9332 (59%)	391 (58%)	103 (42%)	70 (43%)
$\phi_{\ell\ell} < 45$	59 (9.2%)	11 (26%)	1649 (18%)	65 (17%)	14 (13%)	10 (15%)

Table 5: The expected number of events for an integrated luminosity of  $1 \text{ fb}^{-1}$  for the signal with Higgs masses between 120 and 160 GeV. The relative efficiency with respect to the previous cut is given in parentheses. The last line shows the total selection efficiency together with the uncertainty from the limited Monte Carlo statistics.

	$H \rightarrow WW$ $m_H = 120 \text{ GeV}$	$H \rightarrow WW$ $m_H = 130 \text{ GeV}$	$H \rightarrow WW$ $m_H = 140 \text{ GeV}$	$H \rightarrow WW$ $m_H = 150 \text{ GeV}$	$H \rightarrow WW$ $m_H = 160 \text{ GeV}$
$\sigma \times \text{BR}(e, \mu, \tau) [\text{fb}]$	560	1060	1570	1970	2330
L1+HLT	247 (44%)	511 (48%)	802 (51%)	1077 (55%)	1353 (58%)
2 lep, $ \eta  < 2$ , $p_t > 20 \text{ GeV}$ $\sigma_{\text{IP}} > 3$ , $ \Delta z_{\text{lep}}  < 0.2 \text{ cm}$	30 (12%)	88 (17%)	171 (21%)	264 (25%)	359 (27%)
$E_t^{\text{miss}} > 50 \text{ GeV}$	12 (39%)	37 (42%)	88 (52%)	150 (57%)	240 (67%)
$\phi_{\ell\ell} < 45$	6.6 (55%)	20 (53%)	44 (50%)	76 (51%)	139 (58%)
$12 \text{ GeV} < m_{\ell\ell} < 40 \text{ GeV}$	5.5 (83%)	15 (76%)	34 (76%)	56 (73%)	107 (77%)
Jet veto	2.3 (41%)	7.4 (50%)	17 (49%)	29 (52%)	56 (52%)
$30 \text{ GeV} < p_t^{\ell \text{max}} < 55 \text{ GeV}$	1.6 (72%)	5.0 (68%)	13 (77%)	23 (80%)	49 (89%)
$p_t^{\ell \text{min}} > 25 \text{ GeV}$	0.80 (49%)	3.2 (63%)	8.2 (64%)	17 (75%)	42 (85%)
$\varepsilon_{\text{tot}}$	$(0.14 \pm 0.03)\%$	$(0.30 \pm 0.04)\%$	$(0.52 \pm 0.05)\%$	$(0.86 \pm 0.07)\%$	$(1.80 \pm 0.06)\%$